AD-A147 436 AN EVALUATION OF AN ADVECTION FOG PREDICTION MODEL(U) 1/1
AIR FORCE GEOPHYSICS LAB HANSCOM AFB MA J WEYMAN
06 JUN 84 AFGL-TR-84-0162

UNCLASSIFIED F/G 4/2 NL

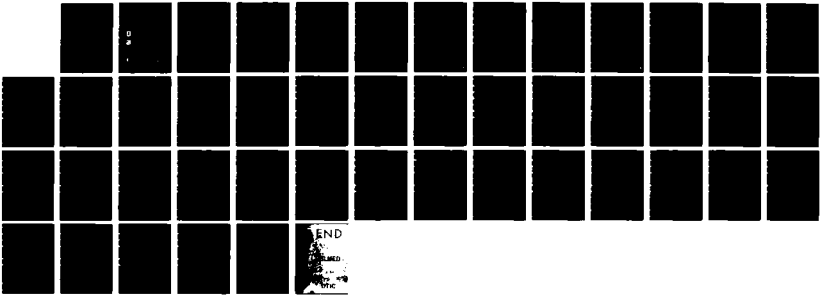

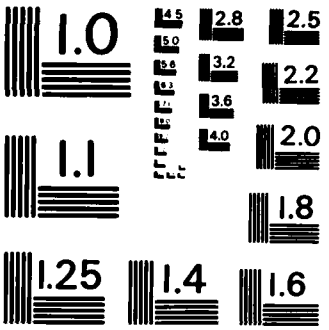

MICROCOPY RESOLUTION TEST CHART
NATIONAL BUREAU OF STANDARDS-1963-A

AFGL-TR-84-0162
ENVIRONMENTAL RESEARCH PAPERS, NO. 883

An Evaluation of an Advection Fog Prediction Model

JAMES WEYMAN, Maj, USAF

6 June 1984

Approved for public release; distribution unlimited.

ATMOSPHERIC SCIENCES DIVISION PROJECT 6670
AIR FORCE GEOPHYSICS LABORATORY
HANSCOM AFB, MA 01731

This report has been reviewed by the ESD Public Affairs Office (PA) and is releasable to the National Technical Information Service (NTIS).

"This technical report has been reviewed and is approved for publication"

FOR THE COMMANDER

Donald D. Grantham

DONALD D. GRANTHAM
Chief, Tropospheric Structure Branch

Robert A. McClatchey

ROBERT A. McCLATCHEY
Director, Atmospheric Sciences Division

Qualified requestors may obtain additional copies from the Defense Technical Information Center. All others should apply to the National Technical Information Service.

If your address has changed, or if you wish to be removed from the mailing list, or if the addressee is no longer employed by your organization, please notify AFGL/DAA, Hanscom AFB, MA 01731. This will assist us in maintaining a current mailing list.

Do not return copies of this report unless contractual obligations or notices on a specific document requires that it be returned.

Unclassified

SECURITY CLASSIFICATION OF THIS PAGE

REPORT DOCUMENTATION PAGE

1a. REPORT SECURITY CLASSIFICATION: Unclassified	1b. RESTRICTIVE MARKINGS
2a. SECURITY CLASSIFICATION AUTHORITY	3. DISTRIBUTION/AVAILABILITY OF REPORT: Approved for public release; distribution unlimited
2b. DECLASSIFICATION/DOWNGRADING SCHEDULE	
4. PERFORMING ORGANIZATION REPORT NUMBER(S): AFGL-TR-84-0162 ERP, No. 883	5. MONITORING ORGANIZATION REPORT NUMBER(S)
6a. NAME OF PERFORMING ORGANIZATION: Air Force Geophysics Laboratory; 6b. OFFICE SYMBOL (If applicable): LYT	7a. NAME OF MONITORING ORGANIZATION: Air Force Geophysics Laboratory
6c. ADDRESS (City, State and ZIP Code): Hanscom AFB Massachusetts 01731	7b. ADDRESS (City, State and ZIP Code): Hanscom AFB Massachusetts 01731
8a. NAME OF FUNDING/SPONSORING ORGANIZATION; 8b. OFFICE SYMBOL (If applicable)	9. PROCUREMENT INSTRUMENT IDENTIFICATION NUMBER
8c. ADDRESS (City, State and ZIP Code)	10. SOURCE OF FUNDING NOS: PROGRAM ELEMENT NO: 62101F; PROJECT NO: 6670; TASK NO: 14; WORK UNIT NO: 02
11. TITLE (Include Security Classification): An Evaluation of an Advection Fog (Contd)	
12. PERSONAL AUTHOR(S): Weyman, James, Maj, USAF	
13a. TYPE OF REPORT: Scientific Final; 13b. TIME COVERED: FROM Oct 1981 TO Sept 1983; 14. DATE OF REPORT (Yr., Mo., Day): 1984 June 6; 15. PAGE COUNT: 45	
16. SUPPLEMENTARY NOTATION	

17. COSATI CODES			18. SUBJECT TERMS (Continue on reverse if necessary and identify by block number)
FIELD	GROUP	SUB GR	Fog; Fog prediction; Fog model
0401			

19. ABSTRACT (Continue on reverse if necessary and identify by block number)

In response to Air Weather Service requirements, ~~AFGL~~ has been involved in research in the development of mesoscale advection fog prediction techniques. A two-dimensional fog prediction model developed at the Naval Environmental Prediction Research Facility (NEPRF) was selected for evaluation because it can operate on a minicomputer of the size planned for the Air Force's Automated Weather Distribution System (AWDS). Six case studies developed by Calspan Advanced Technology Center were used to test the model's accuracy. These case studies covered a wide range of fog/stratus formation and dissipation stages. Four major weaknesses were identified in the model. The most important was that cloud tops increased in temperature through infrared radiative heat processes rather than decreased. The other weaknesses include lack of solar radiation processes, unreliable treatment of the height of mixed layer during stable conditions, and insufficient handling of vertical motions. The model may have potential in AWDS. However, these weaknesses must first be corrected.

20. DISTRIBUTION/AVAILABILITY OF ABSTRACT: UNCLASSIFIED/UNLIMITED ☒ SAME AS RPT ☐ DTIC USERS ☐	21. ABSTRACT SECURITY CLASSIFICATION: Unclassified
22a. NAME OF RESPONSIBLE INDIVIDUAL: James Weyman	22b. TELEPHONE NUMBER (Include Area Code): (617) 861-2972; 22c. OFFICE SYMBOL: LYT

DD FORM 1473, 83 APR EDITION OF 1 JAN 73 IS OBSOLETE

Unclassified

SECURITY CLASSIFICATION OF THIS PAGE

Block 11 (Contd)
Prediction Model

Preface

The author wishes to thank Mrs. Joan Ward for her sincere assistance in programming the plotting routines and investigating potential trouble areas. This report would not have been possible without her. In addition, the author is grateful for the patient guidance of Bruce Kunkel and the many valuable discussions held with him concerning this project. Lastly, the contributions of two very dedicated individuals, Mrs. Jan McDaniel of the Det 9, 24 Weather Sq, and Mrs. Helen Connell of AFGL of typing and preparing this manuscript are gratefully acknowledged.

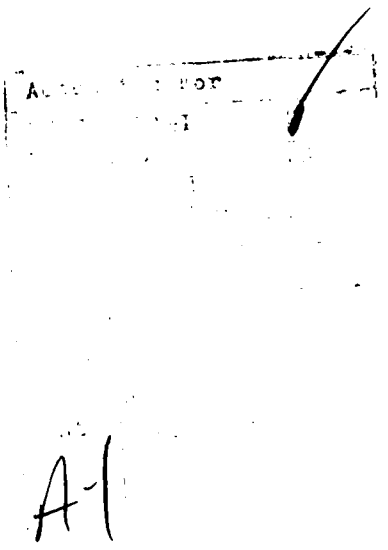

Contents

Illustrations

Illustrations

Tables

An Evaluation of an Advection Fog Prediction Model

1. INTRODUCTION

In response to Geophysical Requirement GR 3-76, the Air Force Geophysics Laboratory (AFGL) has been involved in research to develop short-range advection fog prediction techniques. This research has been a two-pronged study. The first part has concentrated on collecting various types of data at and near the Weather Test Facility at Otis ANGB, Mass., to gain a better understanding of the microphysical and dynamic processes in fog. The results of this work have been reported by Kunkel,[1, 2, 3] Mack,[4] and Hanley et al.[5] The second part of this project was to select an advection fog prediction model and to test its accuracy by com-

(Received for publication 5 June 1984)

1. Kunkel, B.A. (1981) Comparison of Fog Drop Size Spectra Measured by Light Scattering and Impaction Techniques, AFGL-TR-81-0049, AD A100252.

2. Kunkel, B.A. (1982) Microphysical Properties of Fog at Otis AFB, AFGL-TR-82-0026, AD A119928.

3. Kunkel, B.A. (1984) Parameterization of droplet terminal velocity and extinction coefficient in fog models, J. Climate Appl. Meteorol. 23:80-89.

4. Mack, E.J., Wattle, B.J., Rogers, C.W., and Pilie, R.J. (1980) Fog Characteristics at Otis AFB, MA., Calspan Corporation Final Report, AFGL-TR-80-0340, AD A095358.

5. Hanley, J.T., Mack, E.J., Wattle, B.J., and Kile, J.N. (1983) The Feasibility of Using Precursor Aerosol Parameters to Predict Visibility in Fog and Haze, Calspan Corporation Final Report, AFGL-TR-83-0195, AD A137141.

paring the model's results with observed case studies. Then, based on the results of this comparison, methods to improve the model would also be sought.

Historically, researchers first had the facilities to develop realistic numerical models of the atmosphere in the late 1950s and early 1960s. These initial efforts focused on many different areas. Blair et al,[6] Lilly,[7] Ogura,[8] and others were simulating buoyant convection. Ogura and Charney[9] developed a model of a squall line, and Orville[10] was investigating mountain upslope winds. In the area of the atmospheric boundary layer, Estoque[11, 12] simulated diurnal temperature variations, while Fisher and Caplan[13] predicted the development and dissipation of fog. A classic paper by Lilly[14] discussed models of cloud-topped mixed layers. Since these primitive beginnings, many researchers using hundreds of models have studied the atmospheric boundary layer and fog/stratus systems. These researchers have tested and examined such items as higher order turbulence closure techniques, methods to handle the entrainment of dry air from above an inversion, short- and long-wave radiation effects, three-dimensional models, moisture inputs, subsidence, exchange coefficients based on model variables, and surface boundary layer fluxes. However, with the increased complexity of certain models and with the addition of a third dimension, much more computer memory and time was necessary. With the technical advances in computer hardware, however, the cost of this larger computing power has decreased.

In this research, the selection of the model to be used was based on three requirements: (1) the memory requirement, which could not exceed that of a minicomputer; (2) atmospheric dynamics, which must be sufficiently sophisticated to

---

6. Blair, A., Metropolis, N., von Neumann, J., Taub, A.H., and Tsingou, M. (1959) The evolution of a convective element: A numerical calculation, in The Atmosphere and the Sea in Motion, Rockefeller Institute Press, New York, pp. 425-439.
7. Lilly, D.K. (1962) On the numerical simulation of buoyant convection, Tellus, 14:148-172.
8. Ogura, Y. (1962) Convection of isolated masses of a buoyant fluid: A numerical calculation, J. Atmos. Sci. 19:492-502.
9. Ogura, Y., and Charney, J.F. (1960) A numerical model of thermal convection in the atmosphere, Proc. Intern. Symp. Numerical Weather Prediction, Tokyo, Japan Meteorol. Soc., 431-451.
10. Orville, H.D. (1964) On mountain upslope winds, J. Atmos. Sci. 21:622-633.
11. Estoque, M.A. (1959) A preliminary report on a boundary layer numerical experiment, GRD Research Notes, AFCRC (ARDC) 20:1-29.
12. Estoque, M.A. (1963) A numerical model of the atmospheric boundary layer, J. Geophys. Res. 68:1103-1113.
13. Fisher, E.L., and Caplan, P. (1963) An experiment in numerical predictions of fog and stratus, J. Atmos. Sci. 20:425-431.
14. Lilly, D. (1968) Models of cloud-topped mixed layers under a strong inversion, Quart. J. Roy. Meteorol. Soc. 94:292-309.

produce realistic results; and (3) availability of the computer code. The first requirement was necessary because the model, after development, was intended to be tested in AFGL's Man-computer Interactive Display Access System (McIDAS), a test bed for Air Weather Service planned Automated Weather Distribution System (AWDS).

The model selected was one developed by Barker[15] at the Naval Environmental Prediction Research Facility (NEPRF). Section 2 of this paper briefly describes the model and a few programming errors discovered in the review of the model. Section 3 details the sensitivity studies done on Barker's basic model and the comparison with his results. Section 4 describes the results of a comparison between the model and six case studies that Calspan Advanced Technology Center developed for the Naval Air System Command. The suggestions and conclusions for this model are listed in Section 5.

2. MODEL DESCRIPTION

The model consists of three distinct levels as shown in Figure 1: the surface boundary layer, the Ekman Layer, and the free atmosphere. The surface bound-

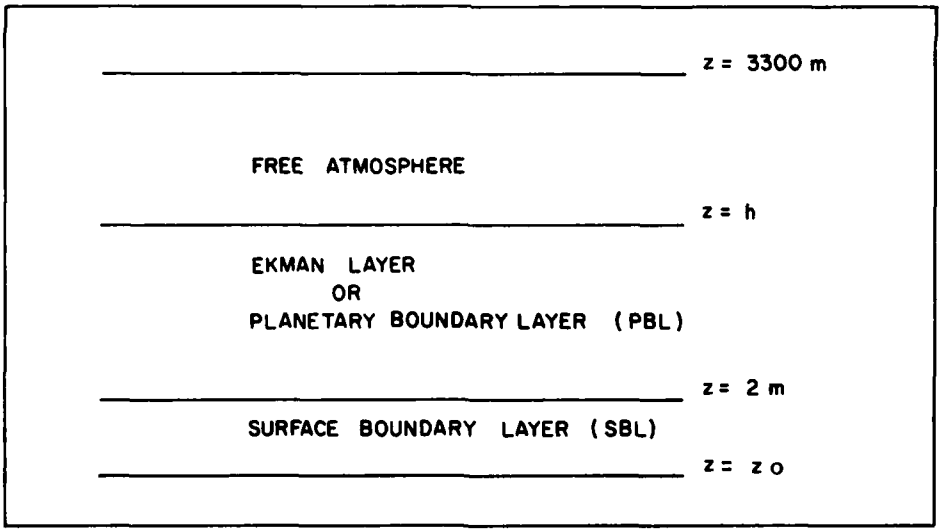

Figure 1. Layers Depicted in Model

15. Barker, E.H. (1977) A maritime boundary-layer model for the prediction of fog, Boundary-Layer Meteorol. 11;267-294.

ary layer (SBL) extends from the surface roughness height, z_o, to a height of 2 m. In this layer, the fluxes of heat, momentum, and moisture are assumed constant. In addition, these fluxes are obtained from the flux gradient similarity relations that permit the fluxes to be described from known mean profiles (Businger[16]). The Ekman layer, or planetary boundary layer (PBL), extends from the top of the SBL (2 m) to the base of the free atmosphere. In this model, the top of the Ekman layer for unstable conditions is defined as the base of the inversion capping the PBL. For a stable layer, the top is empirically determined. It is assumed that the PBL is in a nonsteady state, is over homogeneous terrain, remains incompressible, and has nondivergent flow. At its top, the turbulent friction gradually diminishes to zero. The PBL layer is topped by the free atmosphere, which is in geostrophic balance.

Only the basic equations for the mathematical relations for the model are provided here. For a more detailed description, see Barker[15, 17] and Barker and Baxter.[18]

2.1 Model Equations

The basic equations to be used in this model are Eq. (1), the horizontal equation of motion; Eq. (2), equation of continuity; Eq. (3), a thermodynamic equation; and Eqs. (4) and (5), conservation of water vapor and liquid water equations.

$$\frac{\partial v}{\partial t} = i f (v_g - v) + \frac{\partial}{\partial z} (\overline{w' u_j'}) \tag{1}$$

$$\frac{\partial u}{\partial x} + \frac{\partial w}{\partial z} = 0 \tag{2}$$

$$\frac{\partial \sigma}{\partial t} = -u \frac{\partial \sigma}{\partial x} - w \frac{\partial \sigma}{\partial z} + \frac{\partial}{\partial z} (\overline{\sigma' w'}) + \frac{R}{\rho} \tag{3}$$

$$\frac{\partial q}{\partial t} = -u \frac{\partial q}{\partial x} - w \frac{\partial q}{\partial z} + \frac{\partial}{\partial z} (\overline{q' w'}) - \frac{C}{\rho} \tag{4}$$

---

16. Businger, J.A. (1973) Turbulent transfer in the atmospheric surface layer, Workshop on Micrometeorology, D.A. Haugan, Ed., Am. Meteorol. Soc.

17. Barker, E.H. (1975) A Maritime Boundary Layer Model for the Prediction of Fog, ENVPREDRSCHFAC Technical Paper No. 4-75.

18. Barker, E.H., and Baxter, T.L. (1975) A note on the computations of atmospheric surface layer fluxes for use in numerical modeling, J. Appl. Meteorol. 14:620-622.

$$\frac{\partial \ell}{\partial t} = -u \frac{\partial \ell}{\partial x} - w \frac{\partial \ell}{\partial z} + \frac{\partial}{\partial z} (\overline{\ell' w'}) + \frac{C}{\rho} + v_t \frac{\partial \ell}{\partial z} \quad (5)$$

Moist static energy, σ, is given by

$$\sigma = C_p T + g z + L q \quad (6)$$

In Eqs. (1) to (6), the definitions of the symbols are:

- C_p specific heat during isobaric processes
- C rate of condensation
- f coriolis parameter
- g acceleration due to gravity
- i square root of -1
- ℓ mixing ratio of liquid water
- L coefficient of latent heating
- q specific humidity
- R radiational heating rate
- t time
- T temperature
- u x-component of velocity
- $\tilde{V}$ velocity vector on complex plane
- $\tilde{V}_g$ geostropic velocity vector on complex plane
- V_t terminal velocity
- w vertical velocity
- x horizontal coordinate
- z vertical coordinate
- ρ air density

The formulation for the surface boundary layer fluxes is fashioned after Businger et al,[19] and eddy exchange coefficients derived by O'Brien[20] were used for turbulent mixing in the PBL. The depth of the PBL during unstable conditions

---

19. Businger, J.A., Wyngaard, J.C., Isumi, Y., and Bradley, E.F. (1971) Flux-profile relationships in the atmospheric surface layer, J. Atmos. Sci. 28:181-189.

20. O'Brien, J.J. (1970) A note on the vertical structure of the eddy exchange coefficient in the planetary boundary layer, J. Atmos. Sci. 27:1213-1315.

is an adaptation of Randall and Arakawa.[21] For stable conditions, the depth is determined empirically after Clarke.[22]

The radiation model is a modified version of the radiation model developed by Atwater[23] which describes the upward and downward diffuse radiation flux at some reference level. In this formulation, the transmissivity effects of clouds, water vapor, and carbon dioxide is calculated, and a cooling/heating rate is found from the net flux divergence.

2.2 Numerical Considerations

The numerical differencing schemes used in this model are the Crank-Nicholson scheme for vertical transport and the momentum equation, upstream differencing for horizontal advection, one-sided differencing at the boundaries, and explicit centered differencing for radiational cooling.

The grid spacing in the horizontal is 10 km; in the vertical, the spacing expands with height. There are 20 vertical columns and 28 levels. The time step used to compute the vertical transport has a maximum value of 2 minutes, but allows the time step for radiational cooling and horizontal transport to be 10 times larger. This was designed to take advantage of the largest time step possible in each process.

The initial values for $\tilde{V}$ are assumed steady state and neutrally stable, and are calculated as described by Kraus.[24] This prevents oscillating solutions.

2.3 Coding Errors

In the analysis of AFGL's copy of this model and its coding, a number of errors were discovered. It was confirmed with Barker (private correspondence) that these errors were also in the original model. The effects of these errors will be discussed in Section 3.

---

21. Randall, D., and Arakawa, A. (1974) A Parameterization of the Planetary Boundary Layer for Numerical Models of the Atmosphere (unpublished).
22. Clarke, R.H. (1970) Recommended methods for the treatment of the boundary layer in numerical models, Australian Meteorol. Magazine, 18:51-71.
23. Atwater, M.A. (1970) Investigation of the Radiation Balance for Polluted Layers of the Urban Environment, Ph.D. thesis, New York University, New York.
24. Kraus, E.B. (1972) Atmosphere-Ocean Interaction, Clarendon Press, Oxford.

3. MODEL COMPARISON AND SENSITIVITY

After a thorough investigation of the model, we attempted to duplicate Barker's results[15] to ensure that we had a current version of the model and that it could reproduce his findings.

Figure 2 is the temperature profile at three locations that Barker reported for

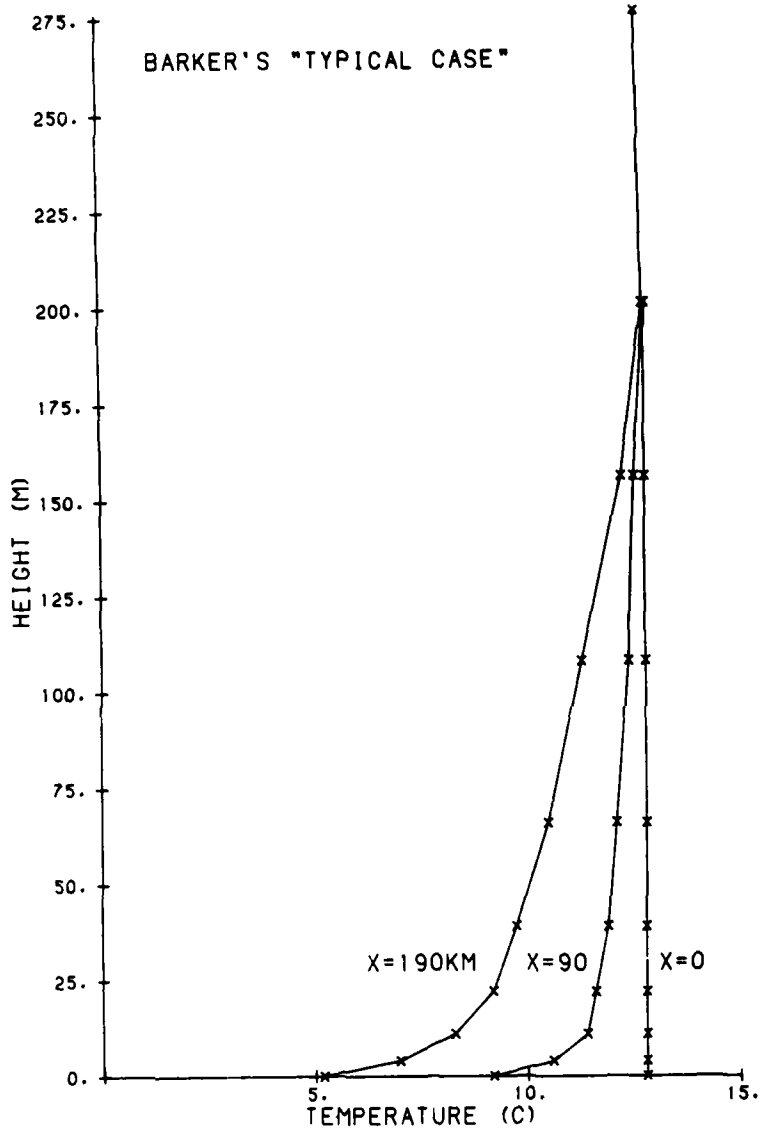

Figure 2. Temperature Profile of "Typical Case" at Three Locations (After Barker[15])

his "typical case." Figure 3 depicts the liquid water content (LWC) profiles in the resulting fog. In this typical case, warm, moist air was advected over cool water. Barker specified a $-0.04°C\,km^{-1}$ sea surface temperature gradient, a geostrophic wind speed of $4\,m\,s^{-1}$ in the x-direction, and temperature and humidity profiles at the upstream boundary that were held constant. Figures 2 and 3 show that the atmosphere cools below 200 m and fog forms near the sea surface and slowly deepens downstream.

To duplicate these results, AFGL's version of Barker's model was run, first in its original form (with coding errors) and then with the corrected coding errors

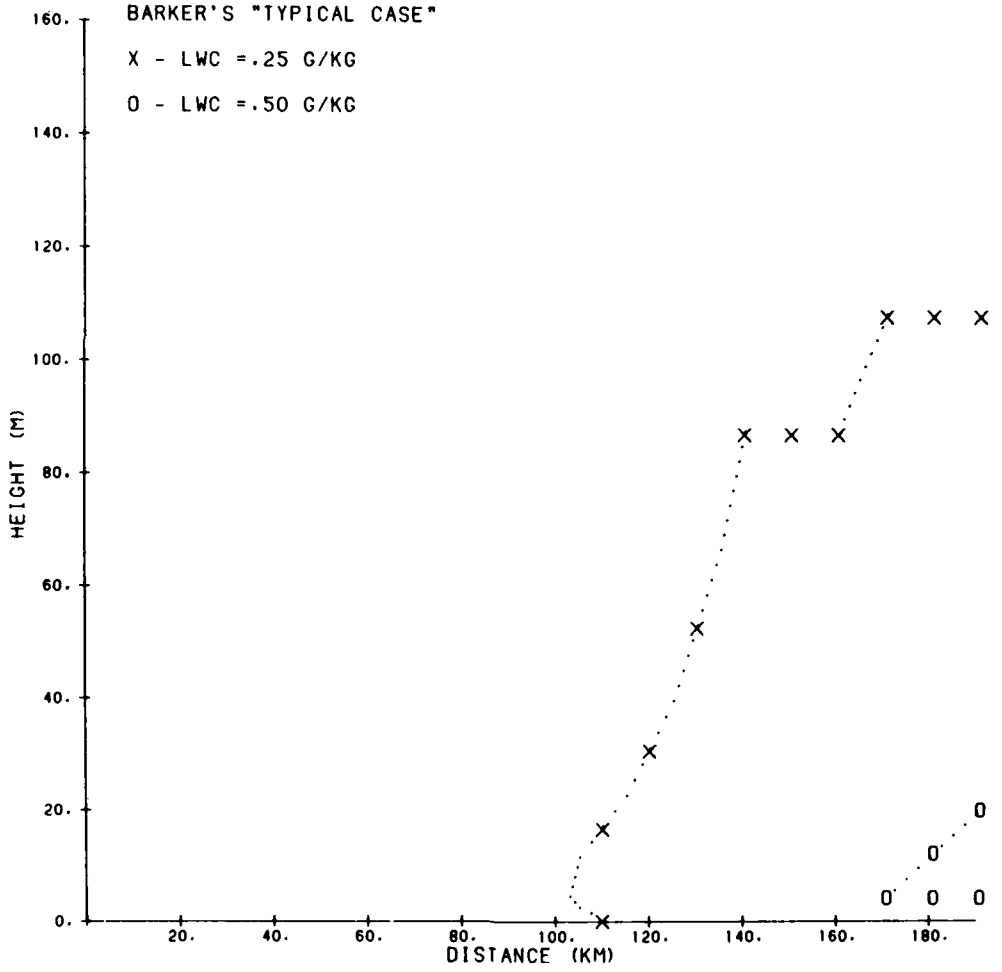

Figure 3. Liquid Water Content (LWC) Values Resulting From "Typical Case" (After Barker[15])

mentioned in Section 2.3. For the typical case, the results are shown in Figures 4 and 5. In the AFGL version (with coding errors), we see that the data agree

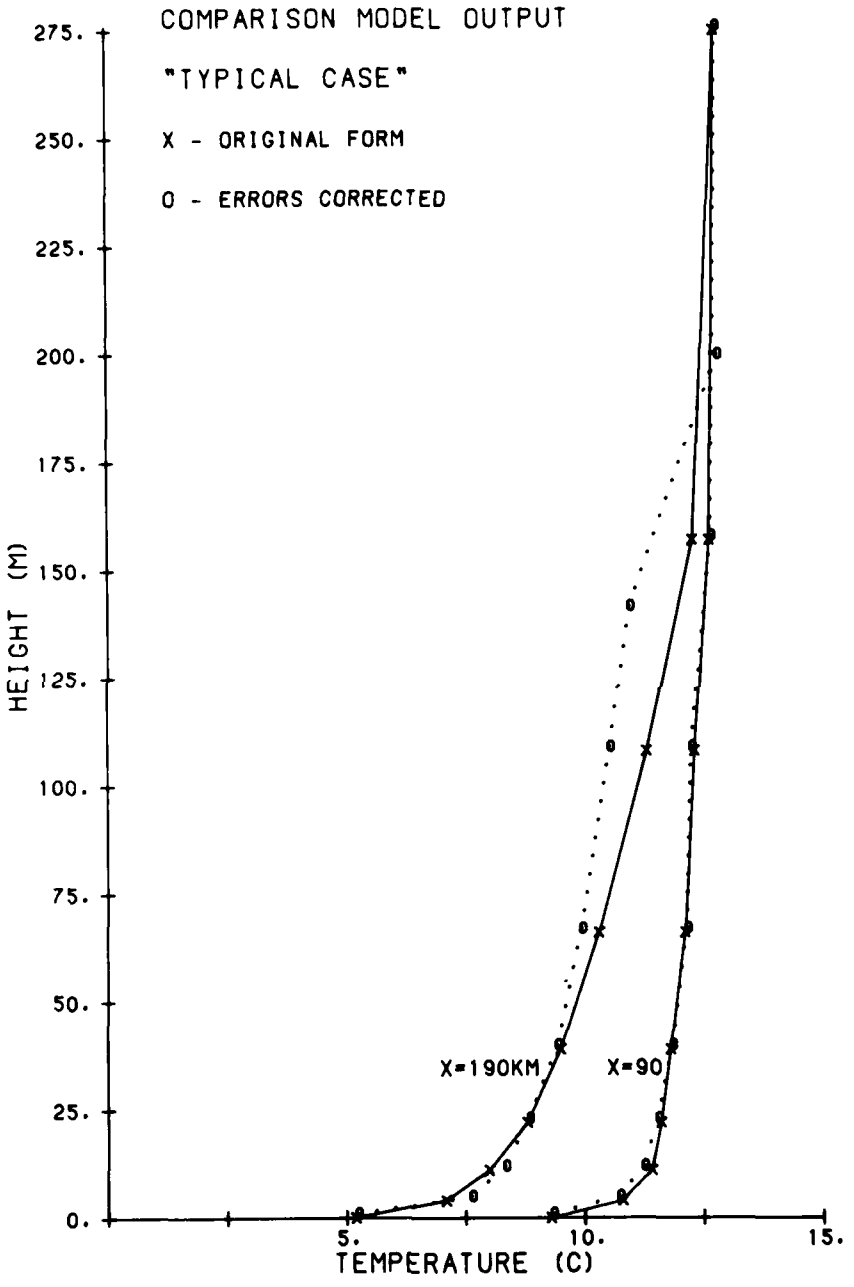

Figure 4. Temperature Profile of "Typical Case" at Two Locations, AFGL Version

very closely with Barker's version (Figure 2) except at x = 190 km, where the temperatures below 200 m are slightly warmer (less than 1°) in Barker's version. With the coding errors corrected, we note very little change at x = 90 km from AFGL's version with the coding errors. However, at x = 190 km, we see slightly warmer temperatures below 25 m and significantly colder (2°) temperatures above that level compared with the AFGL version with the coding errors.

For the formation of fog, a comparison of Figures 3 and 5 points out the differences. The AFGL model in the original form developed fog at the same location

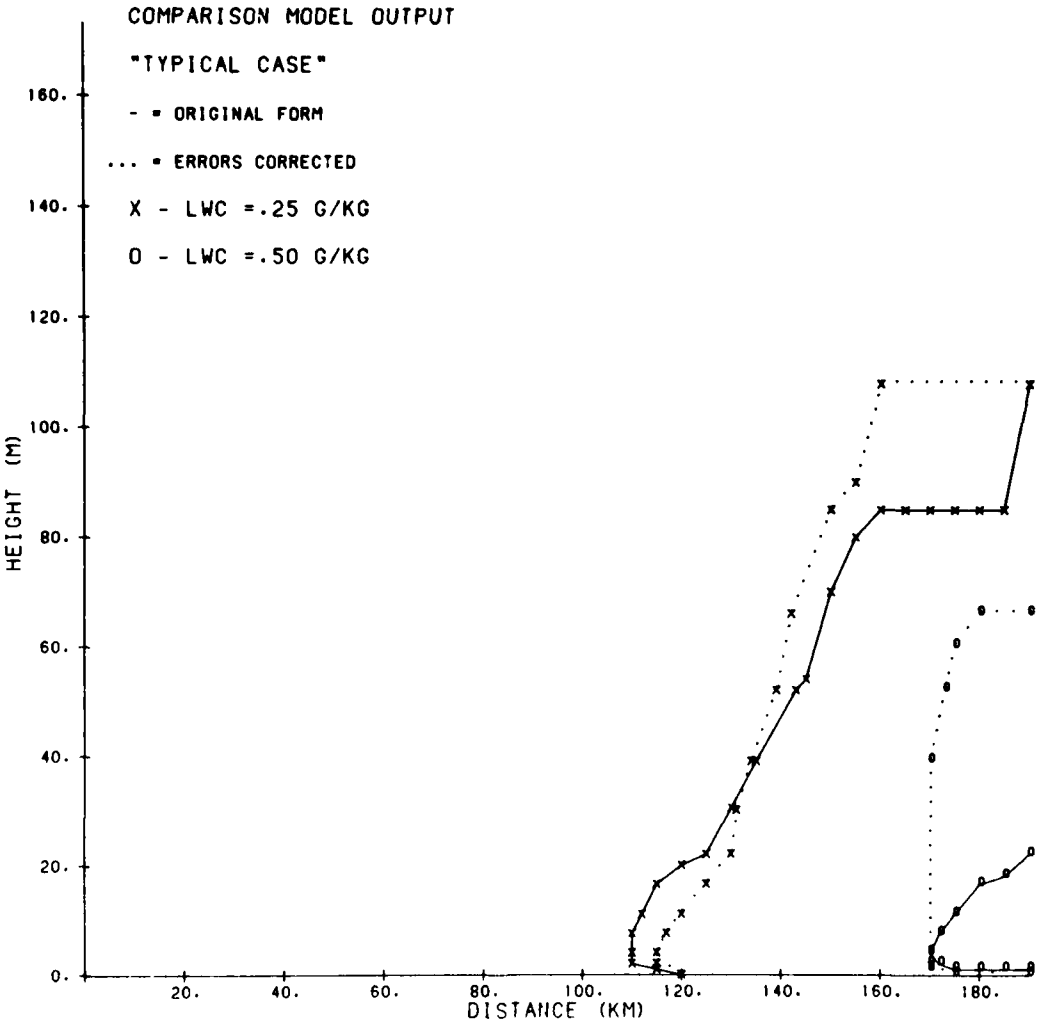

Figure 5. Liquid Water Content (LWC) Values Resulting From "Typical Case," AFGL Version

(110 km) as Barker reported; however, the vertical extent was lower than in Barker's version. The opposite is true when we compare LWCs greater than 25 g kg^{-1}. The starting point for both is the same, but the vertical extent of the larger LWCs is slightly greater for the AFGL original form than for Barker's. The AFGL corrected model output shows the fog developing slightly farther downstream and a much larger vertical extent of the larger values of LWC than in either of the original versions.

Based on the above comparison and the small differences between the AFGL original form model and the data Barker reported, it was assumed that AFGL's original version of the model was very similar to Barker's.

After an analysis of the coding errors that were discovered, we determined that the error of primary importance was in the calculation of the delta virtual potential temperature, $\Delta\theta_v$. The model calculates the bulk Richardson Number from the $\Delta\theta_v$. Then the model uses the bulk Richardson Number to determine the surface boundary layer fluxes and the eddy exchange coefficients. When we corrected this error, the surface boundary layer fluxes increased slightly, and the eddy exchange coefficients increased moderately. The result was to increase the diffusion of cold, moist air near the water surface to greater heights. Therefore, as shown in Figures 4 and 5, the corrected model had colder temperatures above 25 m, greater vertical extent to the fog, and higher LWCs than either of the original versions.

In another experiment, Barker considered the atmosphere to be adiabatic above 200 m while all other conditions remained as they were in the typical case. This greatly increased the amount of net radiation leaving the boundary layer. Figures 6 and 7 (after Barker) display the results of this experiment. A comparison of this case with the typical case (Figures 2 and 3) shows that the fog is more extensive, the LWCs are higher, and the temperatures below 200 m at x = 190 km are considerably colder than in the typical case.

The output from the AFGL original and corrected models for this experiment is shown in Figures 8 and 9. Again, we see a close correlation between Barker's data and the original form data (see Figures 6 and 7). However, this time we see very little difference between the AFGL original and corrected form data. Because of the expanding vertical grid, the errors appear large above 80 m, but, in fact, represent a difference of only one grid interval. In this case, the cooling was very large because of the net radiation loss near the fog's top. It completely dominated the diffusion effects. Therefore, the errors introduced by the coding problem were minimal in comparison with the overall results.

Barker[17] described a number of other experiments he performed. These involved studying the model's sensitivity to moisture, wind speed, and sea surface temperature gradient. Each experiment he listed was tested both in the AFGL ori-

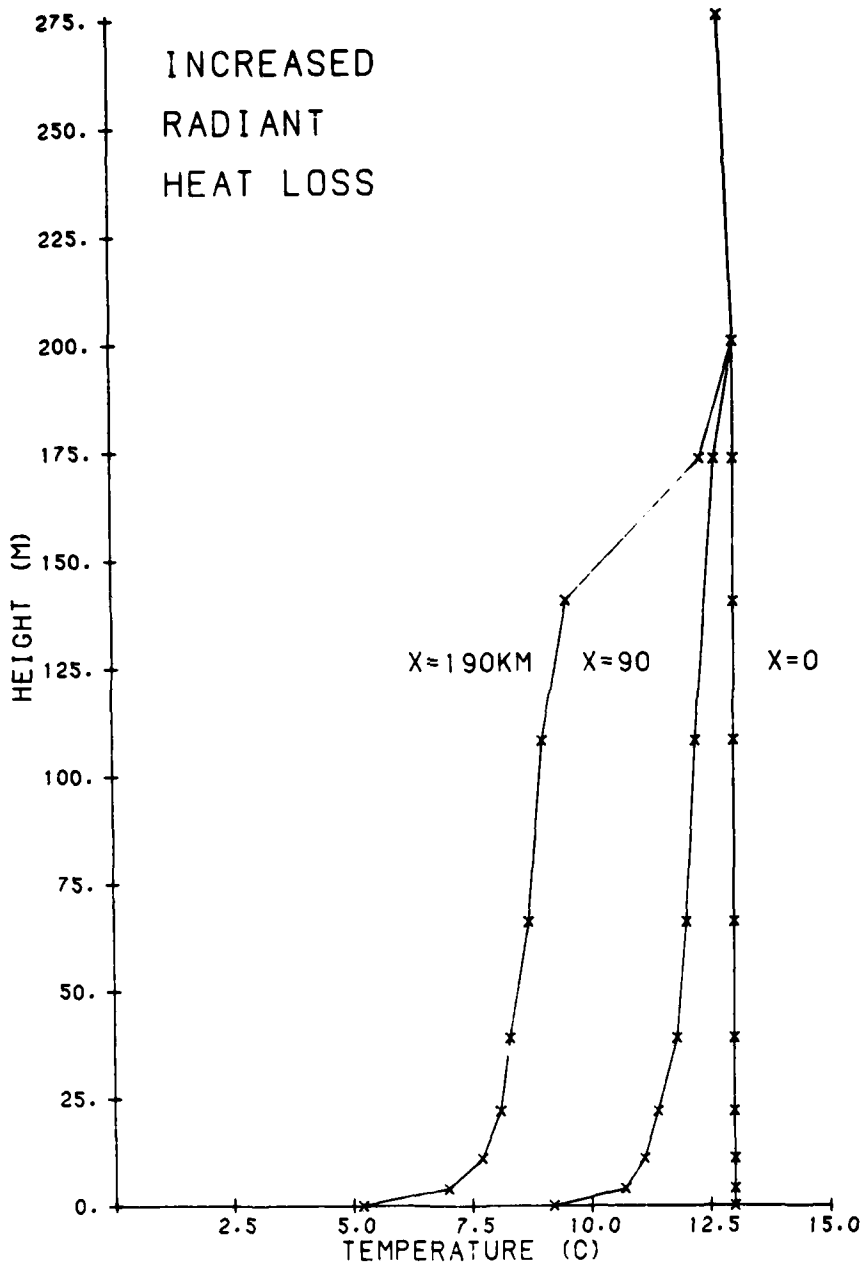

Figure 6. Temperature Profile of Increased Radiant Heat Loss Case at Three Locations (After Barker[15])

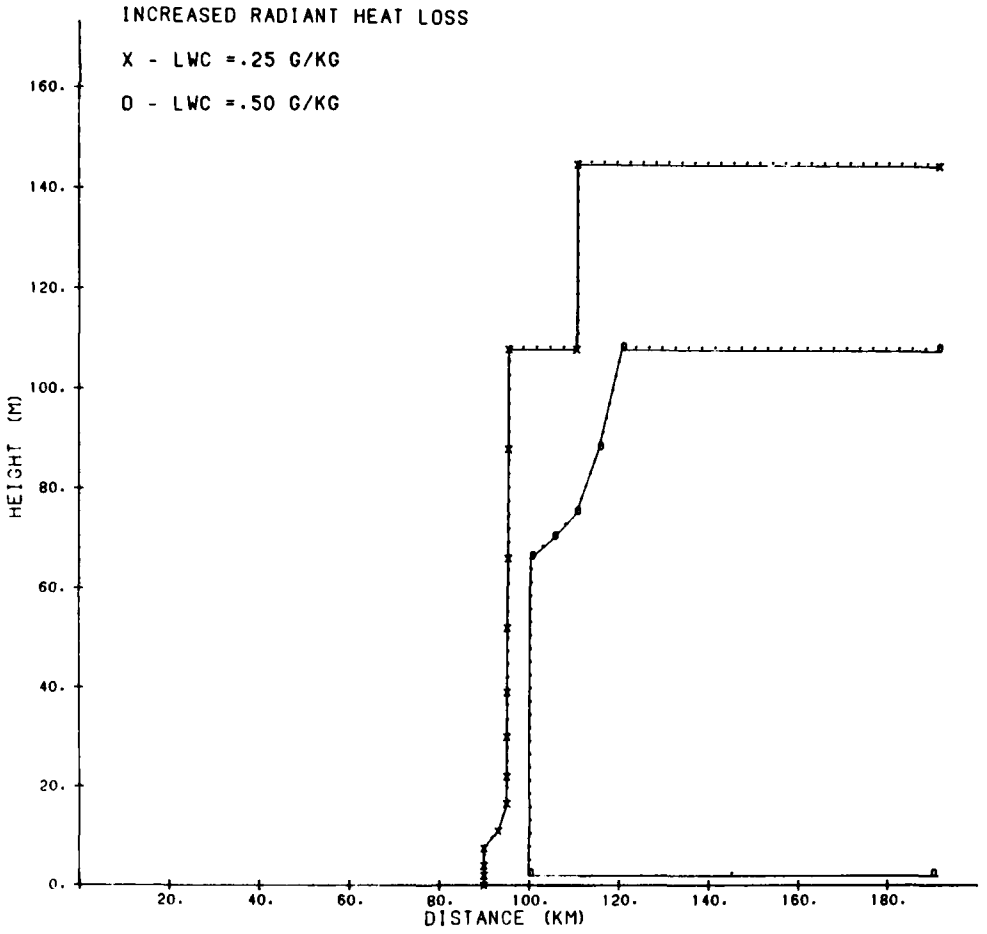

Figure 7. Liquid Water Content (LWC) Values Resulting From Increased Radiant Heat Loss Case (After Barker[15])

ginal and the corrected models. The original model results compared quite well with Barker's results for each of these. For the corrected version, results similar to those discussed in this section were found. When turbulent diffusion effects played an important part, large differences occurred between the original and corrected forms. When diffusion was dominated by other effects, then both versions closely agreed.

4. RESULTS

When AFGL initiated its research into short-range fog prediction techniques,

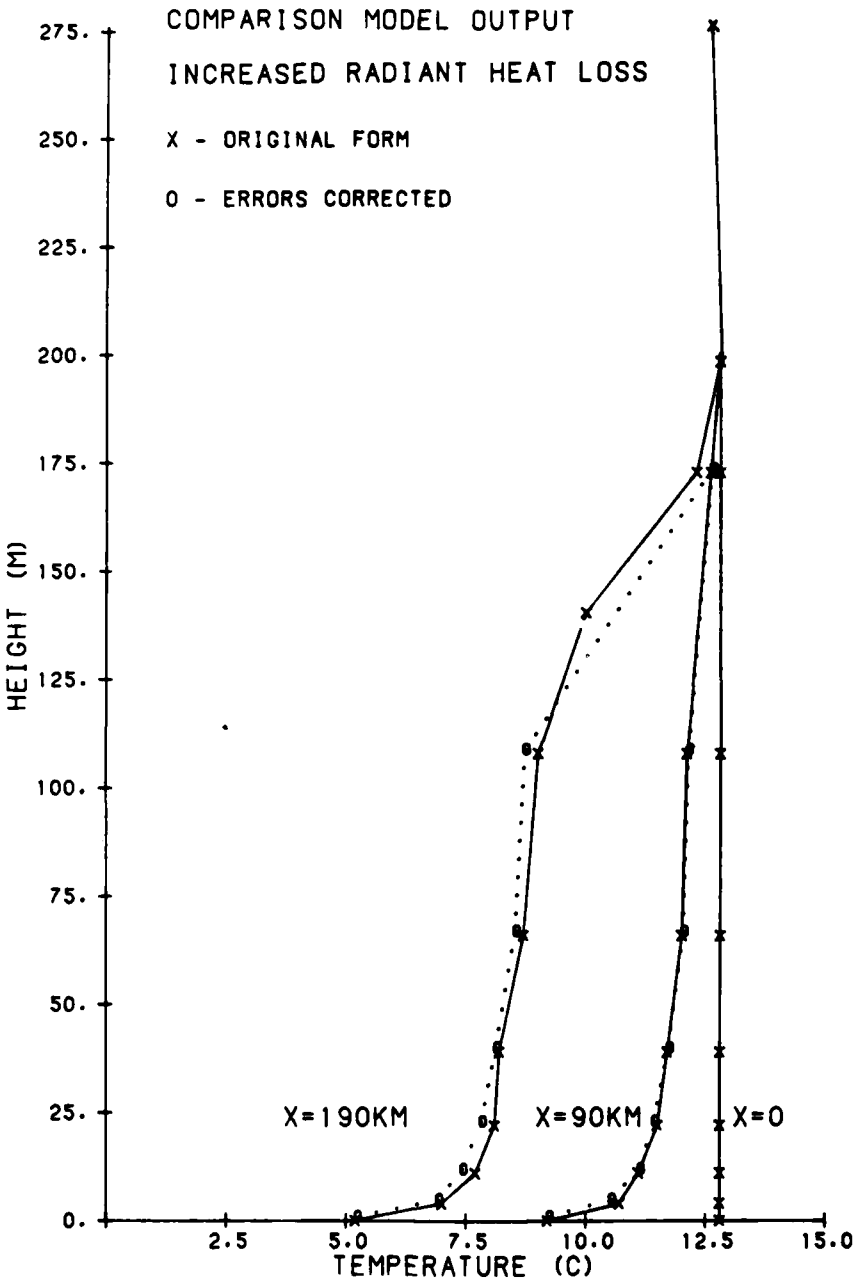

Figure 8. Temperature Profile of Increased Radiant Heat Loss Case at Three Locations, AFGL Version

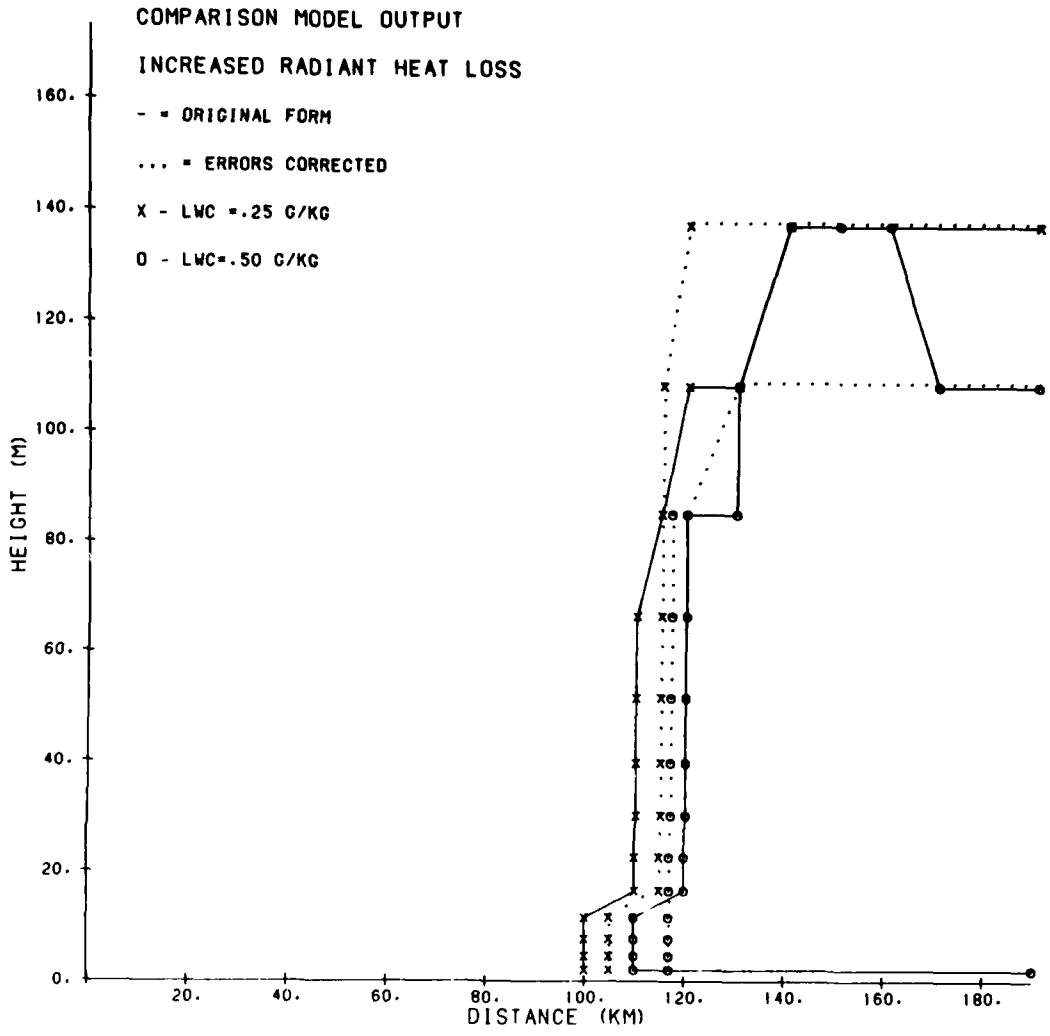

Figure 9. Liquid Water Content (LWC) Values Resulting From Increased Radiant Heat Loss Case, AFGL Version

the plan was to test the effectiveness of the selected two-dimensional fog prediction model with data obtained at Otis ANGB, Mass. AFGL[1, 2, 3] and Calspan[4, 5] under contract to AFGL collected the necessary surface data at and upwind of Otis ANGB. However, fine-scale vertical sounding data did not become available until late in the measurement program, when there were no suitable fog cases.

At approximately the same time, under a 2-year contract (No. N00019-81-C-0102) with the Naval Air Systems Command, Calspan Advanced Technology Center was assembling information derived from recent marine fog observations and anal-

yzing various models for marine fog and the marine boundary layer. Their goal was to develop operationally useful forecast concepts. Under Task 1 of this effort, Calspan provided six data sets with which various numerical model investigators could exercise their models. Table 1 is a summary of those six data sets.

These data sets provided the necessary vertical and horizontal meteorological variables to conduct realistic tests on the AFGL's selected two-dimensional model. In addition, the six cases covered a variety of situations that enabled strong and weak points of the model to be identified. The model's temperature and dew point output results from each of these cases were plotted against the initial and verification profiles and are presented in Appendix A. A summary of the initial data and the model output and verification data is presented in Table 2.

The outcome of the comparison between the verification data and the model data was very disappointing. The model did not develop one episode of fog or lowering stratus in any of the six cases. In Cases 1, 3, 4, and 6, where a cloud layer was initially specified, the model rapidly evaporated the liquid water, produced 100 percent relative humidities below the temperature inversions, and then changed very little for the remaining time period. The model was then examined to seek reasons for the poor performance. Four areas were found that adversely affected the results.

4.1 Net Flux Divergence of Infrared Radiation

Case 6 is an evening situation where initially stratus is reported from 100-200 m. After 3 hours, the entire layer below 200 m cools and the depth of the fog is observed from the surface to 200 m. In Figures A11 and A12, we can see that, instead of cooling, the model warmed the entire layer and evaporated the existing liquid water cloud droplets.

The procedure used in the model for handling the net flux divergence of the infrared radiation was examined to find an explanation for this occurrence. This flux divergence is directly proportional to the cooling/heating rate of the atmosphere. For Case 6, the cooling rate for the cloud top vertical grid interval (36 m thick) was calculated. Instead of finding a positive value (cooling), the first 20-min period produced a cooling rate of -1.75°C/h (net warming). In the next lower vertical grid interval (30 m thick), which was completely filled by cloud, the cooling rate was -0.7°C/h.

To verify this result, temperature and flux profiles from Flight 8 on 12 May 1976 (Stephens et al[25]) were used as input into the model. In the cloud top vertical grid interval (cloud 80 m thick in interval), the rate was -0.5°C/h. In the grid interval below this (100 m thick), which was completely filled by cloud, the cooling rate was -1.1°C/h. Although Stephens et al did not report the specific cooling rate

for this flight, on similar flights the upper two layers had IR cooling rates of 1.0 to 2.0°C/h respectively.

The Calspan results and the results from the Stephens et al[25] data showed that the magnitude of the cooling was correct in the model but the sign was incorrect. The method used in the model for handling the IR radiation process was examined in detail, but no obvious procedural errors could be found to explain the results. At one point, it appeared that there was an incorrect sign in the code and, when we changed the sign, good agreement was found with Case 1 and Case 6 as shown in Table 3. However, further examination revealed the sign to be correct. Although the problem could not be pinpointed, this investigation did identify the model's weakness in the IR cooling process.

4.2 Planetary Boundary Layer Depth During Stable Conditions

During stable conditions ($zL^{-1} > 0$), Clarke[22] empirically determined the depth of the PBL to be approximately

$$H = .23u_*/f \tag{7}$$

where u_* is the friction velocity in cm sec^{-1} and f is the coriolis parameter in sec^{-1}. This formulation is used in the model. However, in Case 4, this proved to be a weak point.

In Monin-Obukhov theory of similarity, a scale length, L, is determined based on heat and momentum fluxes in the surface boundary layer. In this model, the surface boundary layer extends from z_o to 2 m. The calculated L is used to determine the stability of the layer. Because of the temperature structure in the lower 2 m for Case 4, the model calculated a stable condition and used Eq. (7) to determine the height of the boundary layer. Based on u_*, the boundary layer height was determined to be 297 m instead of 500 to 560 m as specified in the initial and verification data. The free atmosphere is assumed to exist above the top of the boundary layer and turbulent intensity is assumed to approach zero. This means that the cloud layer that extended from 420 m to 500 m underwent no turbulent change. As a result of IR radiational cooling, the cloud layer warmed slightly and evaporated all the liquid water.

It is interesting to note here that, when the apparent incorrect minus sign in the IR radiational cooling routine was changed (Section 4.1), the results for Cases 1 and 6 improved greatly but those for Case 4 did not. The cloud was not evaporated, but it was not altered (lowered or raised) either. It continued to exist between 420 m to 500 m along the entire horizontal dimension of the model. This was caused by the boundary layer height being fixed at 350 m. Therefore, the cloud existed in

Table 1. Description and Summary of Calspan's Six Data Sets

CASE	TYPE	FORECAST PERIOD (H)	TIME OF DAY	LOW LEVEL TEMP STRUCTURE	INITIAL CLOUD
22 May 1978 Case 1	Stratus/ no stratus	4	Morning	Unstable to Neutral	yes
2 Aug 1975 Case 2	Shallow cold water advection fog	3	Evening	Inverted	no
7 Oct 1976 Case 3	Thinning stratus redeveloping to form fog	10, 14, 20	Morning to Night	Neutral	yes
14-15 July 1973 Case 4	Stratus thickening	10	Night	Neutral	yes
5 Aug 1975 Case 5	Shallow cold water fog deepening over warm water	1-3	Morning	Inverted to Isothermal	no
29 Aug 1972 Case 6	Stratus lowering to fog	3	Evening	Neutral	yes

Table 2. Comparison of Initial and Verification Data From Calspan's Six Sets With Model Output

CASE	INITIAL CLOUD	HEIGHT RANGE (m)	VERIFICATION/MODEL TEMPERATURE DIFFERENTIAL (°C)	DEPTH OF BOUNDARY LAYER (m)		
				Initial	Verification	Model
1a	no	0-800	8 to -1.0	790	850	780
1b	yes	0-800	-0.5 to -1.5	790	850	863
2	no	0-28	-3.0 to -6.0	inverted	inverted	366
3_{10}	yes	0-250	-2.0 to 3.0	270	250	287
3_{14}	yes	0-100	-1.0 to -2.0	270	100	323
3_{20}	yes	0-250	-2.0 to -3.0	270	250	275
4	yes	0-560	0 to +1.0	500	560	297
5_1	no	0-28	+3.0 to +4.2	inverted	inverted	177
5_2	no	0-28	0 to +4.0	inverted	17.5	190
5_3	no	0-30	0 to +4.0	inverted	30	219
cold	yes	0-200	0 to +2.0	200	200	161
warm	yes	0-200	0 to +2.0	200	200	161

Table 1 (contd). Description and Summary of Calspan's Six Data Sets

CASE	WINDS	SYNOPTIC SCALE VERTICAL MOTION	SEA SURFACE TEMP	
			Relative to Air	Trend with Distance
22 May 1978 Case 1	mod	weak upward	warm	warming
2 Aug 1975 Case 2	mod	---------	cold	cooling
7 Oct 1976 Case 3	lt	strong subsidence	warm	warming
14-15 July 1973 Case 4	lt	zero	warm	constant
5 Aug 1975 Case 5	mod	----------	cold to warm	warming
29 Aug 1972 Case 6	lt	zero	warm/ cold	------

Table 2 (contd). Comparison of Initial and Verification Data From Calspan's Six Sets With Model Output

CASE	FOG/CLOUD BASE AND TOP (m)					CLOUD/THICKNESS MAXIMUM LIQUID WATER CONTENT				
	Initial Base/Top		Verification Base/Top		Model Base/Top	Initial Thick (m)	Initial Max LWC (g/m^3)	Verification Thick (m)	Model Thick (m)	Model Max LWC (g/m^3)
1a	688	688	468	800	None	0	0	322	0	None
1b	464	688	468	800	None	224	.36	332	0	None
2	-	-	0	28	None	0	0	28	0	None
3_{10}	144	265	None		None	121	.20	0	0	None
3_{14}	144	265	None		None	121	.20	0	0	None
3_{20}	144	265	44	250	None	121	.20	206	0	None
4	420	500	250	610	None	80	.26	360	0	None
5_1	-	-	0	50	None	0	0	50	0	None
5_2	-	-	0	50	None	0	0	50	0	None
5_3	-	-	0	100	None	0	0	100	0	None
cold	100	200	0	200	None	100	.15	200	0	None
warm	100	200	0	200	None	100	.15	200	0	None

Table 3. Comparison of Verification Data With Model Output for Cases 1 and 6. "Apparent error" in IR radiational cooling routine corrected

	VERIFICATION/MODEL TEMPERATURE DIFFERENTIAL (°C)	DEPTH OF BOUNDARY LAYER (m)		FOG/CLOUD BASE AND TOP (m)		CLOUD THICKNESS (m)	
		Verif	Model	Verif	Model	Verif	Model
1a	-1.0 to -2.0	850	868	468 800	617 868	332	251
1b	-1.0 to -2.0	850	880	468 800	492 880	332	388
6 cold (3 h)	0 to 1.0	200	200	0 200	97 200	200	103
6 cold (5 h)	0 to +0.5		213		0 213		213
6 warm (3 h)	0 to 1.0	200	200	0 200	99 200	200	101
6 warm (5 h)	0 to 0.5		208		0 208		208

the free atmosphere and underwent little change. The boundary layer height determination overwhelmed the "improved" IR cooling effects.

4.3 Vertical Motion

In the model, the vertical motion is derived by integrating the equation of continuity for incompressible, nondivergent flow:

$$w(z) = -\int_0^z \frac{\partial u}{\partial x}\, dz. \tag{8}$$

This is a definite weakness in situations such as Case 3, where strong subsidence plays an important role in the evolution of the atmosphere. In the model under investigation, the initial subsidence cannot be taken into account. For Case 3, this has a significant effect. In addition, because of the complete dependence on $\partial u/\partial x$, the resultant vertical velocity field appears almost random.

4.4 Short Wave Radiation

In Cases 1, 3, and 5, solar radiation effects played an important part in the development/dissipation of the fog and clouds. This model neglects short wave radiation effects. Stephens et al[25] reported in their research that measured short wave flux divergence can be equal in magnitude and sometimes larger than the long wave flux divergence. Therefore, the lack of solar radiation effects is a significant weakness.

5. SUGGESTIONS AND CONCLUSIONS

The results from the numerical model appear to agree very well with the results reported by Barker.[15] This agreement indicates that the model realistically simulates the formation of fog when warm moist air is advected over cold water. The model shows that a stable moist layer, when cooled from below, can form a surface based inversion layer that remains well mixed.

However, as described in Section 4, a minimum of four changes must be made before the model can be used outside of this limited context. These four changes are:

(a) Include solar radiation effects. This would permit diurnal variations.

(b) Include a better treatment of vertical motions and a way to input initial vertical motions. This would permit modeling cases where subsidence plays a large role.

(c) Develop a different method to determine the height of boundary layer for

stable conditions. This task would be easily accomplished and would produce significant benefits.

(d) Modify the infrared radiative transfer equations. This is the most important change of the four. An in-depth review and necessary changes would produce very large benefits.

This model still has potential in an Automated Weather Distribution System (AWDS). However, the weaknesses described in Section 4 must first be corrected. In addition, these improvements must be accomplished keeping in mind the limited storage and processing time of a minicomputer.

References

1. Kunkel, B.A. (1981) Comparison of Fog Drop Size Spectra Measured by Light Scattering and Impaction Techniques, AFGL-TR-81-0049, AD A100252.
2. Kunkel, B.A. (1982) Microphysical Properties of Fog at Otis AFB, AFGL-TR-82-0026, AD A119928.
3. Kunkel, B.A. (1984) Parameterization of droplet terminal velocity and extinction coefficient in fog models, J. Climate Appl. Meteor. 23:80-89.
4. Mack, E.J., Wattle, B.J., Rogers, C.W., and Pilie, R.J. (1980) Fog characteristics at Otis AFB, MA., Calspan Corporation Final Report, AFGL-TR-80-0340, AD A095358.
5. Hanley, J.T., Mack, E.J., Wattle, B.J., and Kile, J.N. (1983) The Feasibility of Using Precursor Aerosol Parameters to Predict Visibility in Fog and Haze, Calspan Corporation Final Report, AFGL-TR-83-0195, AD A137141.
6. Blair, A., Metropolis, N., von Neumann, J., Tuab, A.H., and Tsingou, M. (1959) The evolution of a convective element: A numerical calculation, in The Atmosphere and the Sea in Motion, Rockefeller Institute Press, New York, pp. 425-439.
7. Lilly, D.K. (1962) On the numerical simulation of buoyant convection, Tellus, 14:148-172.
8. Ogura, Y. (1962) Convection of isolated masses of a buoyant fluid: A numerical calculation, J. Atmos. Sci. 19:492-502.
9. Ogura, Y., and Charney, J.F. (1960) A numerical model of thermal convection in the atmosphere, Proc. Intern. Symp. Numerical Weather Prediction, Tokyo, Japan Meteorol. Soc., 431-451.
10. Orville, H.D. (1964) On mountain upslope winds, J. Atmos. Sci, 21:622-633.
11. Estoque, M.A. (1959) A preliminary report on a boundary layer numerical experiment, GRD Research Notes, AFCRC(ARDC) 20:1-29.
12. Estoque, M.A. (1963) A numerical model of the atmospheric boundary layer, J. Geophys. Res. 68:1103-1113.

13. Fisher, E.L., and Caplan, P. (1963) An experiment in numerical predictions of fog and stratus, J. Atmos. Sci. 20:425-431.

14. Lilly, D. (1968) Models of cloud-topped mixed layers under a strong inversion, Quart. J. Roy. Meteorol. Soc. 94:292-309.

15. Barker, E.H. (1977) A maritime boundary-layer model for the prediction of fog, Boundary-Layer Meteorol. 11:267-294.

16. Businger, J.A. (1973) Turbulent transfer in the atmospheric surface layer, Workshop on Micrometeorology, D.A. Haugan, Ed., Am. Meteorol. Soc.

17. Barker, E.H. (1975) A Maritime Boundary Layer Model for the Prediction of Fog, ENVPREDRSCHFAC Technical Paper No. 4-75.

18. Barker, E.H., and Baxter, T.L. (1975) A note on the computations of atmospheric surface layer fluxes for use in numerical modeling, J. Appl. Meteorol. 14:620-622.

19. Businger, J.A., Wyngaard, J.C., Isumi, Y., and Bradley, E.F. (1971) Flux-profile relationships in the atmospheric surface layer, J. Atmos. Sci. 28:181-189.

20. O'Brien, J.J. (1970) A note on the vertical structure of the eddy exchange coefficient in the planetary boundary layer, J. Atmos. Sci. 27:1213-1315.

21. Randall, D., and Arakawa, A. (1974) A Parameterization of the Planetary Boundary Layer for Numerical Models of the Atmosphere (unpublished).

22. Clarke, R.H. (1970) Recommended methods for the treatment of the boundary layer in numerical models, Australian Meteorol. Magazine, 18:51-71.

23. Atwater, M.A. (1970) Investigation of the Radiation Balance for Polluted Layers of the Urban Environment, Ph.D. thesis, New York University, New York.

24. Kraus, E.B. (1972) Atmosphere-Ocean Interaction, Clarendon Press, Oxford.

25. Stephens, G.L., Paltridge, G.W., and Platt, C.M.R. (1978) Radiation profiles in extended water clouds III: Observations, J. Atmos. Sci., 35:2133-2141.

Appendix A

Case Studies

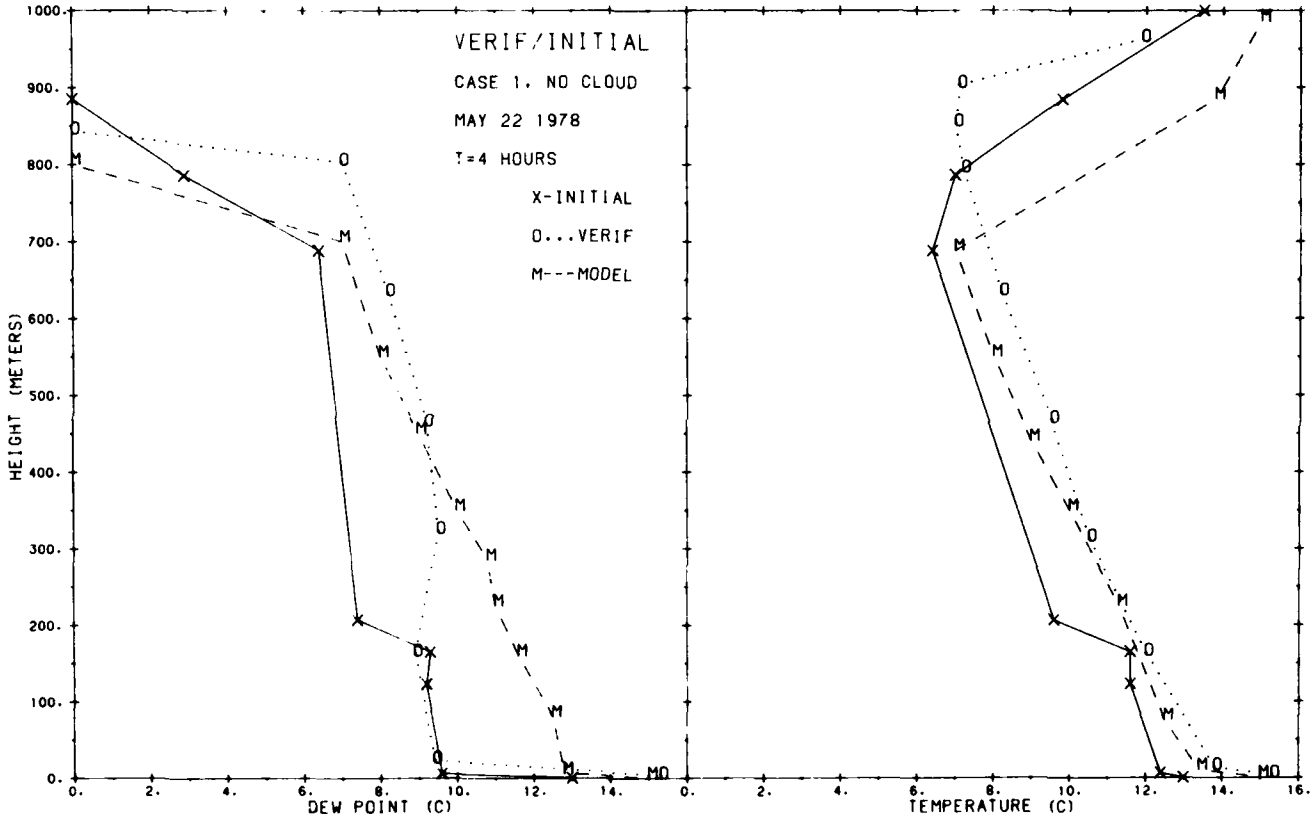

Figure A1. Initial, Verification, and Model Temperature and Dew Point Temperature Profiles for Calspan Case 1 at 4 Hours, No Initial Cloud

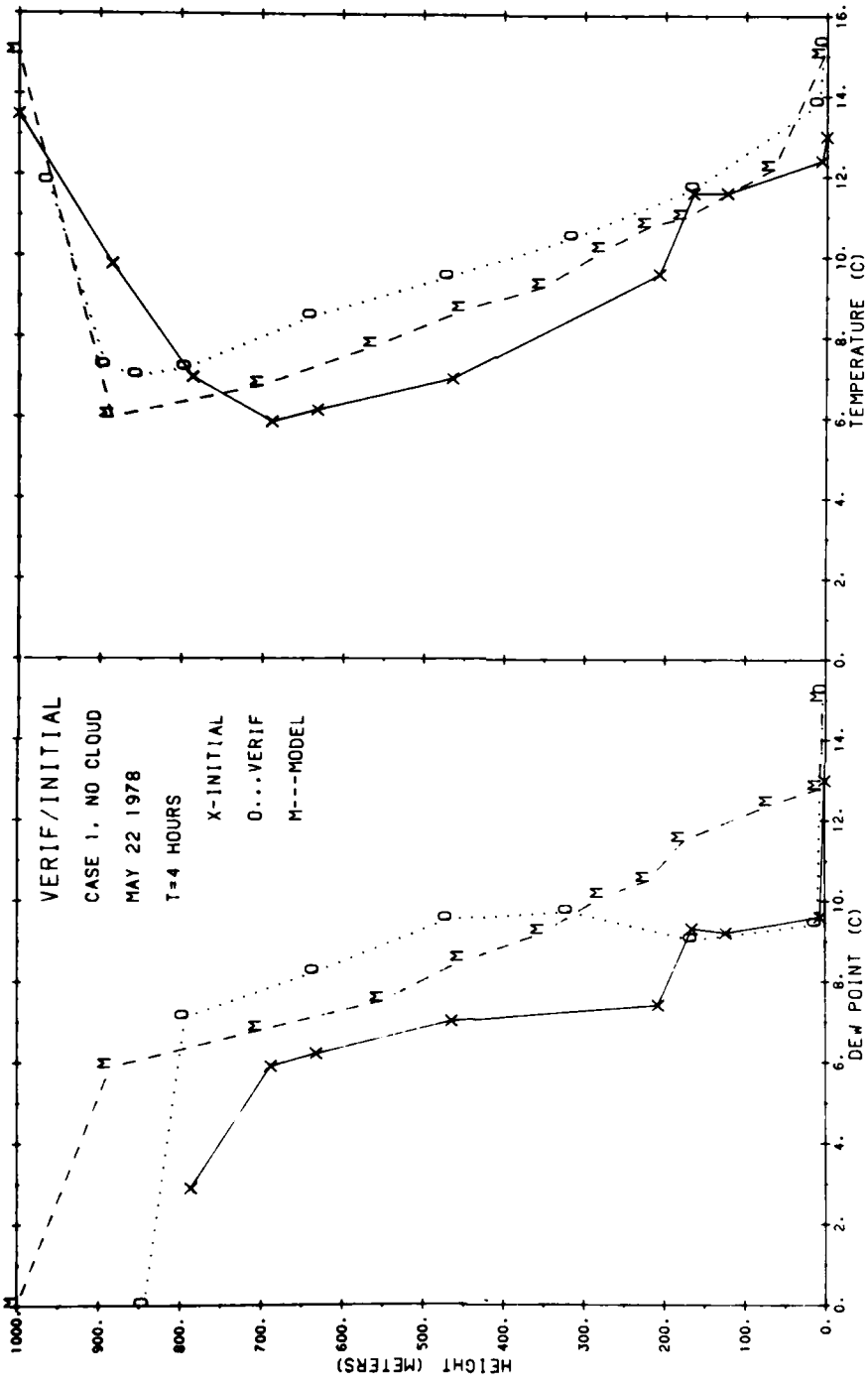

Figure A2. Initial, Verification, and Model Temperature and Dew Point Temperature Profiles for Calspan Case 1 at 4 Hours, Cloud Layer Between 464 m and 688 m

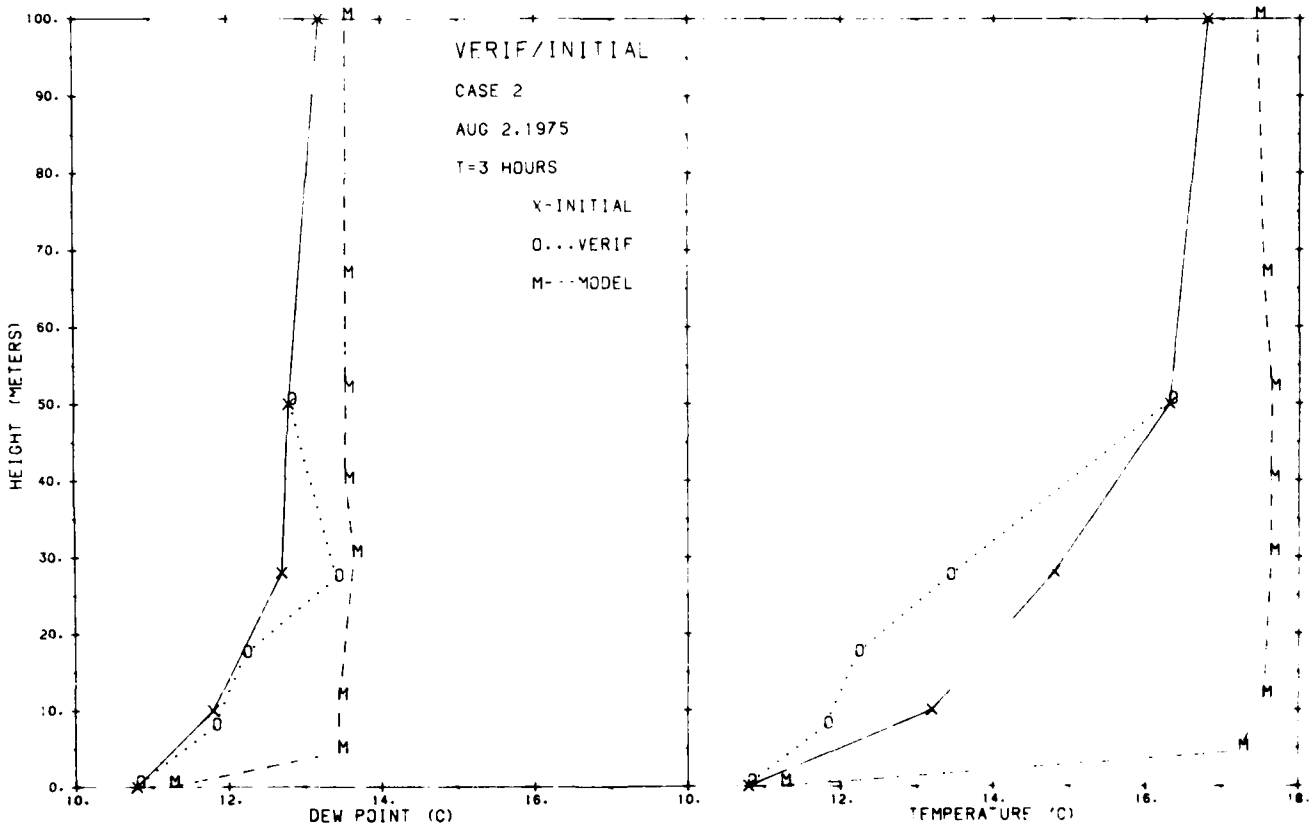

Figure A3. Initial, Verification, and Model Temperature and Dew Point Temperature Profiles for Calspan Case 2 at 3 Hours, No Initial Cloud

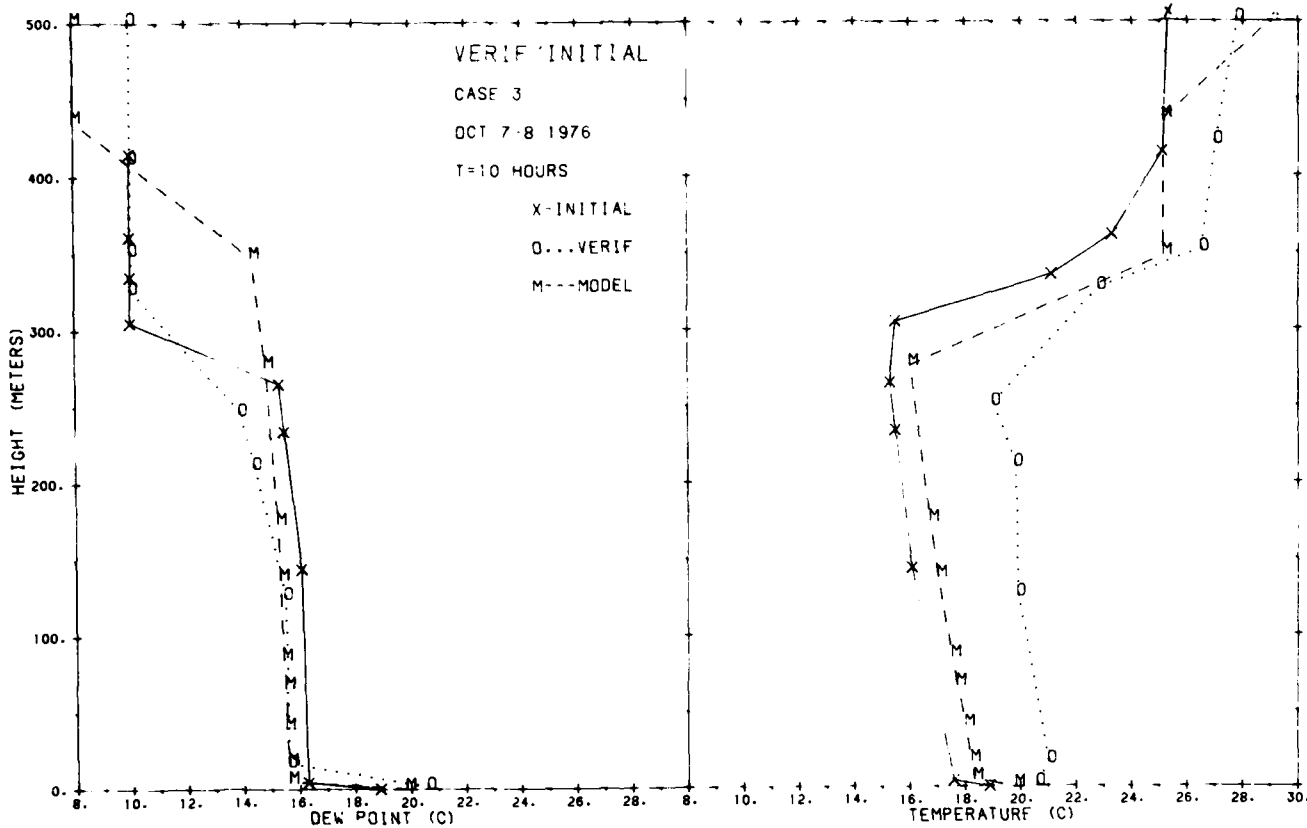

Figure A4. Initial, Verification, and Model Temperature and Dew Point Temperature Profiles for Calspan Case 3 at 10 Hours, Initial Cloud Layer Between 200 m and 265 m

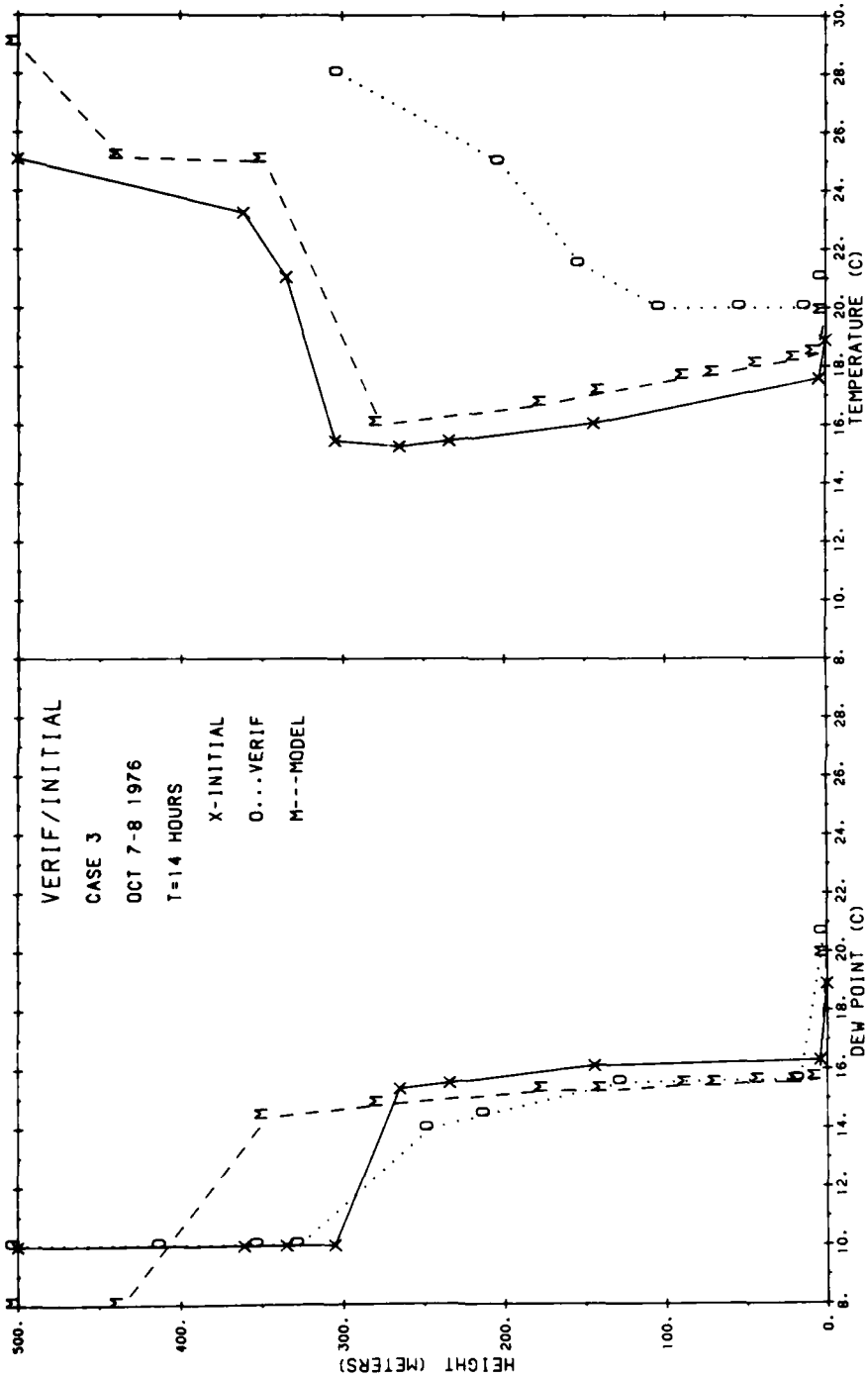

Figure A5. Initial, Verification, and Model Temperature and Dew Point Temperature Profiles for Calspan Case 3 at 14 Hours, Initial Cloud Layer Between 200 m and 265 m

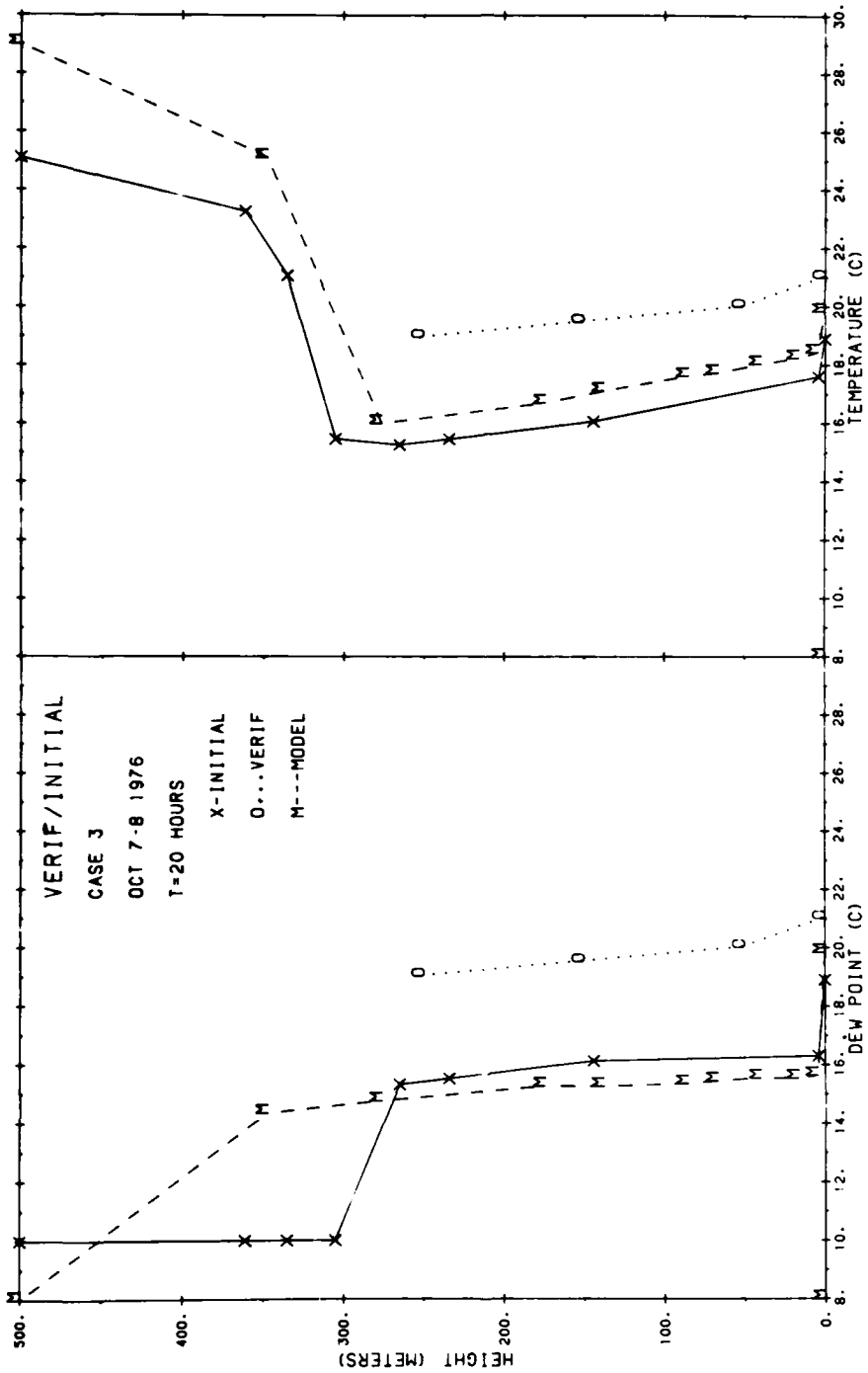

Figure A6. Initial, Verification, and Model Temperature and Dew Point Temperature Profiles for Calspan Case 3 at 20 Hours, Initial Cloud Layer Between 200 m and 265 m

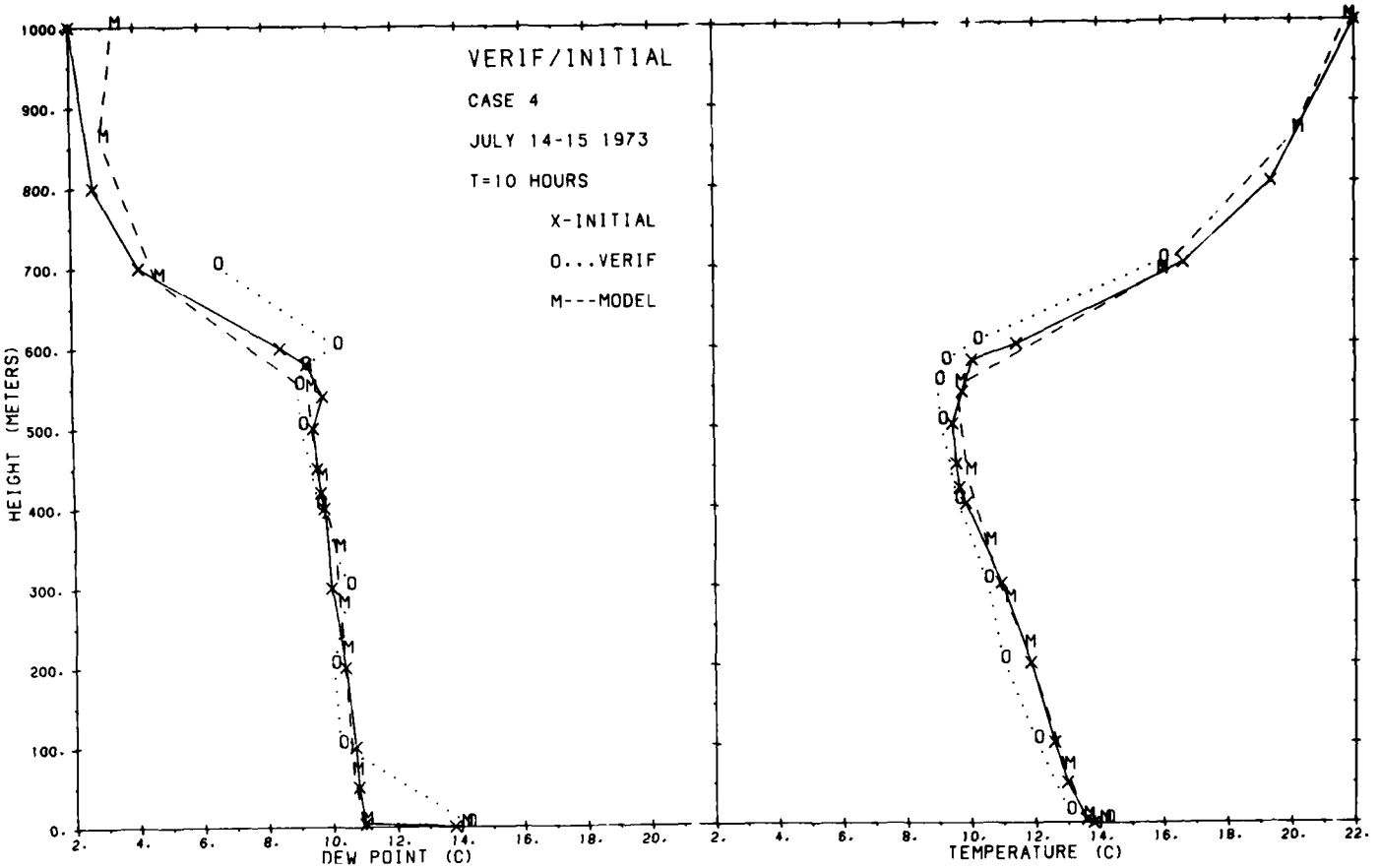

Figure A7. Initial, Verification, and Model Temperature and Dew Point Temperature Profiles for Calspan Case 4 at 10 Hours, Initial Cloud Layer Between 450 m and 540 m

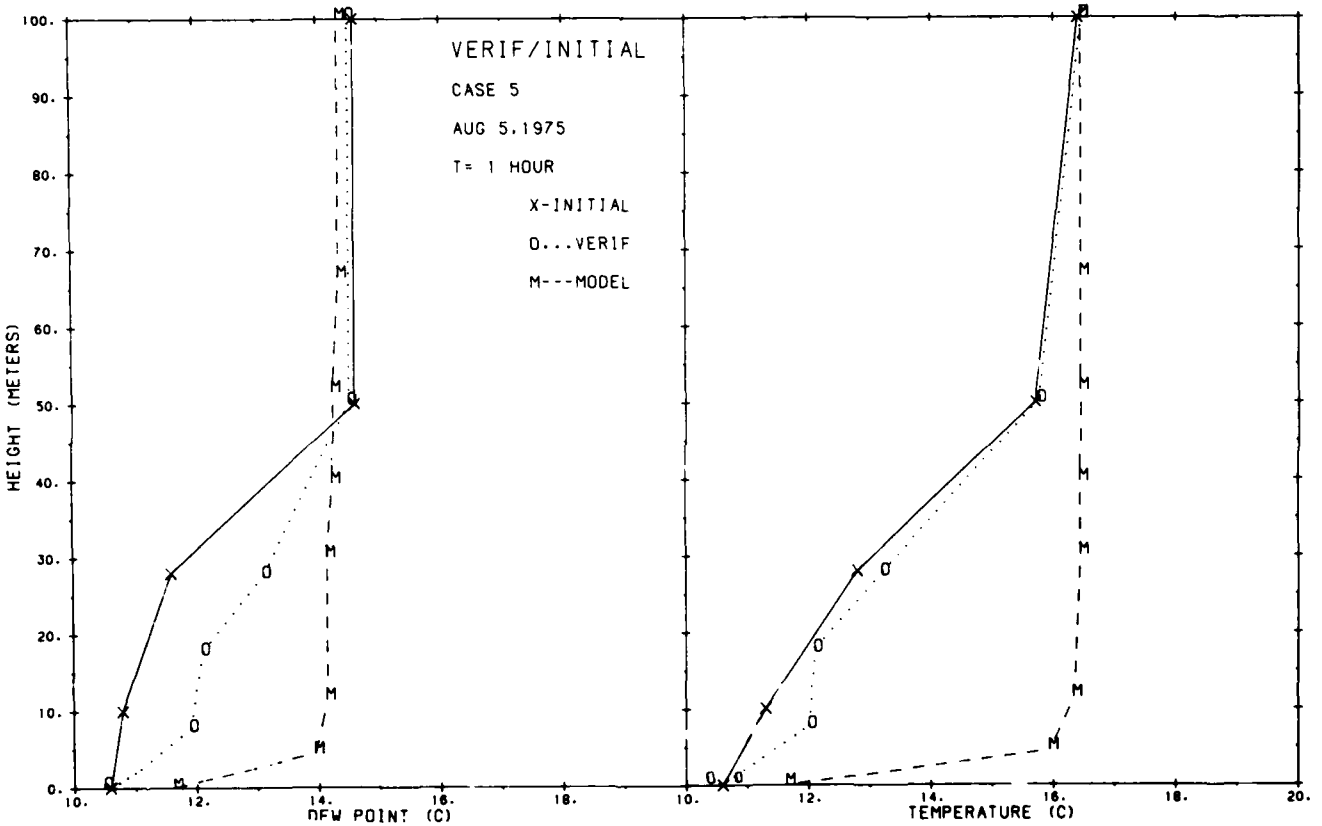

Figure A8. Initial, Verification, and Model Temperature and Dew Point Temperature Profiles for Calspan Case 5 at 1 Hour, No Initial Cloud

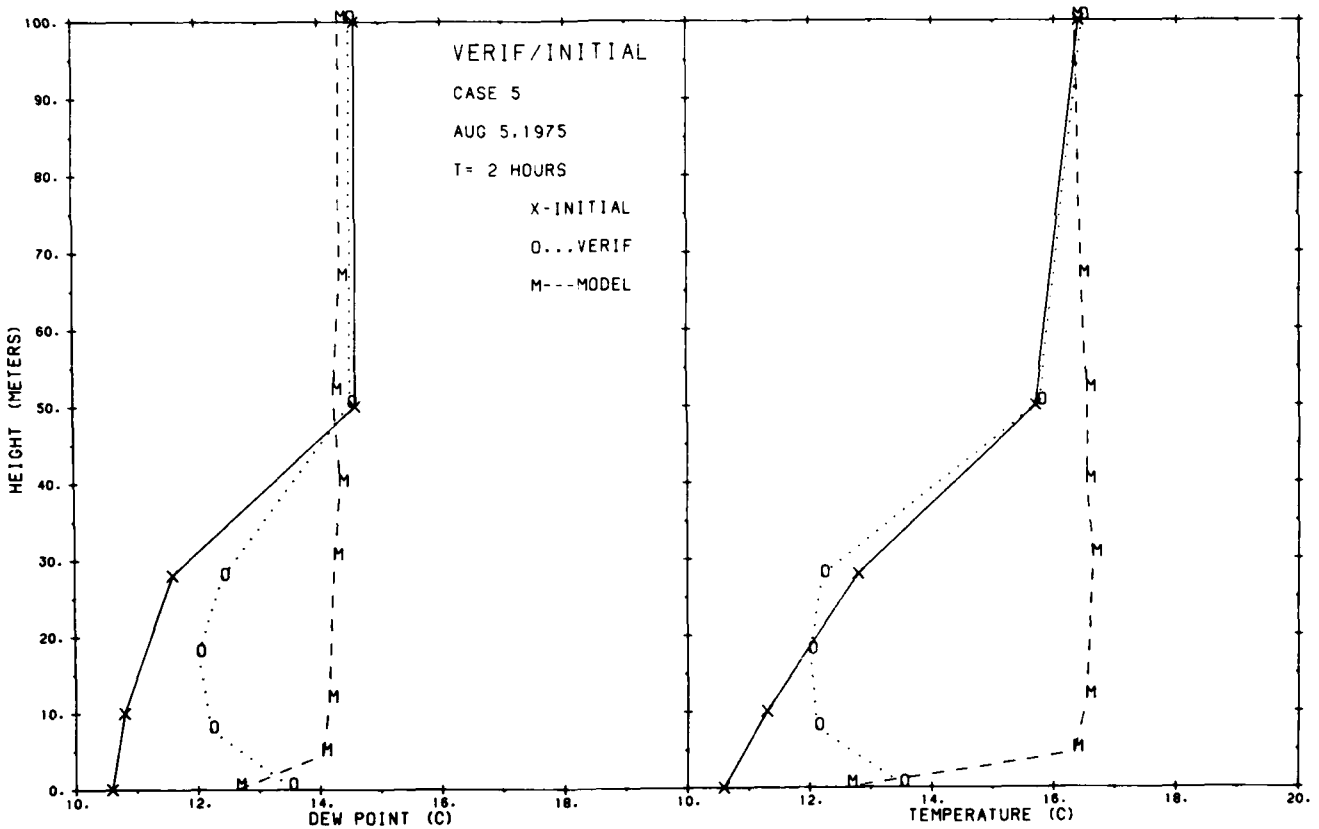

Figure A9. Initial, Verification, and Model Temperature and Dew Point Temperature Profiles for Calspan Case 5 at 2 Hours, No Initial Cloud

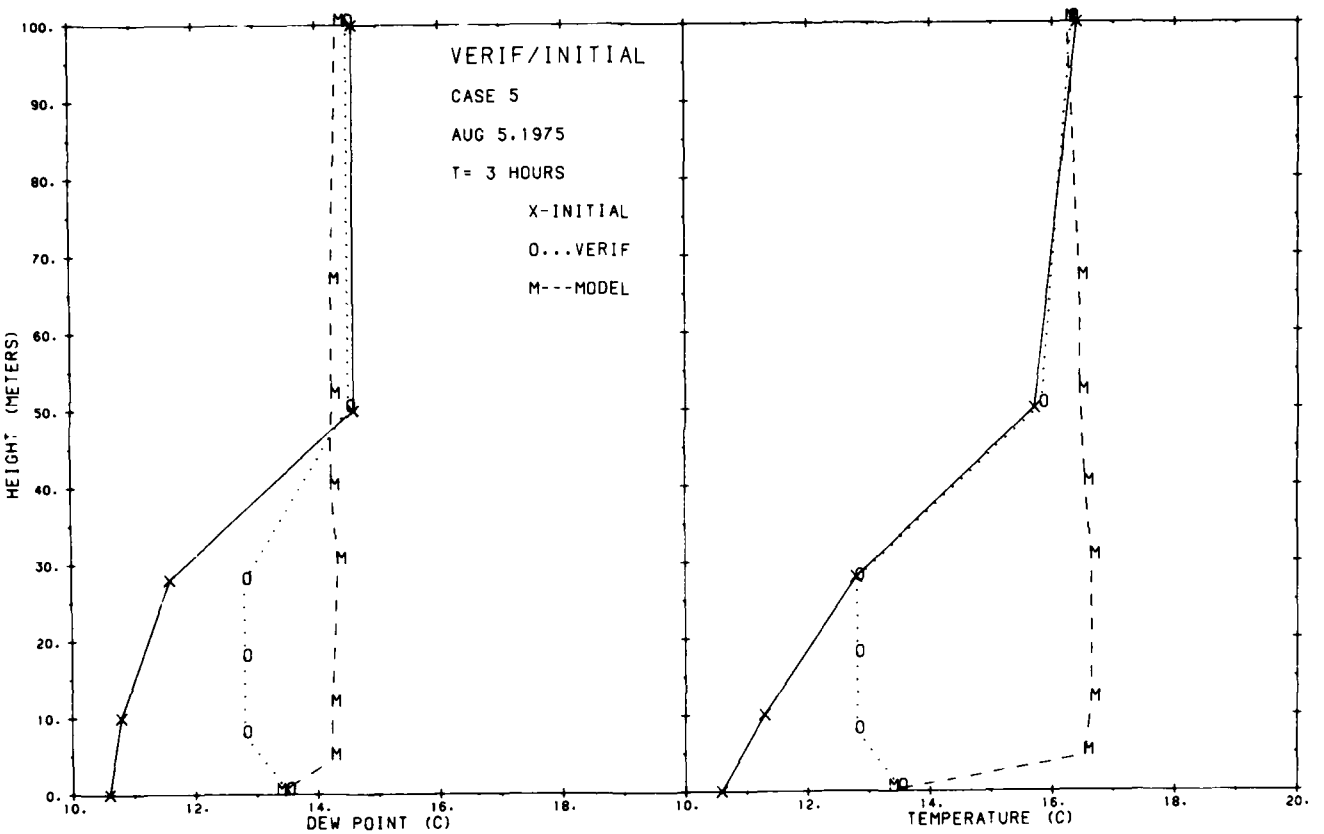

Figure A10. Initial, Verification, and Model Temperature and Dew Point Temperature Profiles for Cuspan Case 5 at 3 Hours, No Initial Cloud

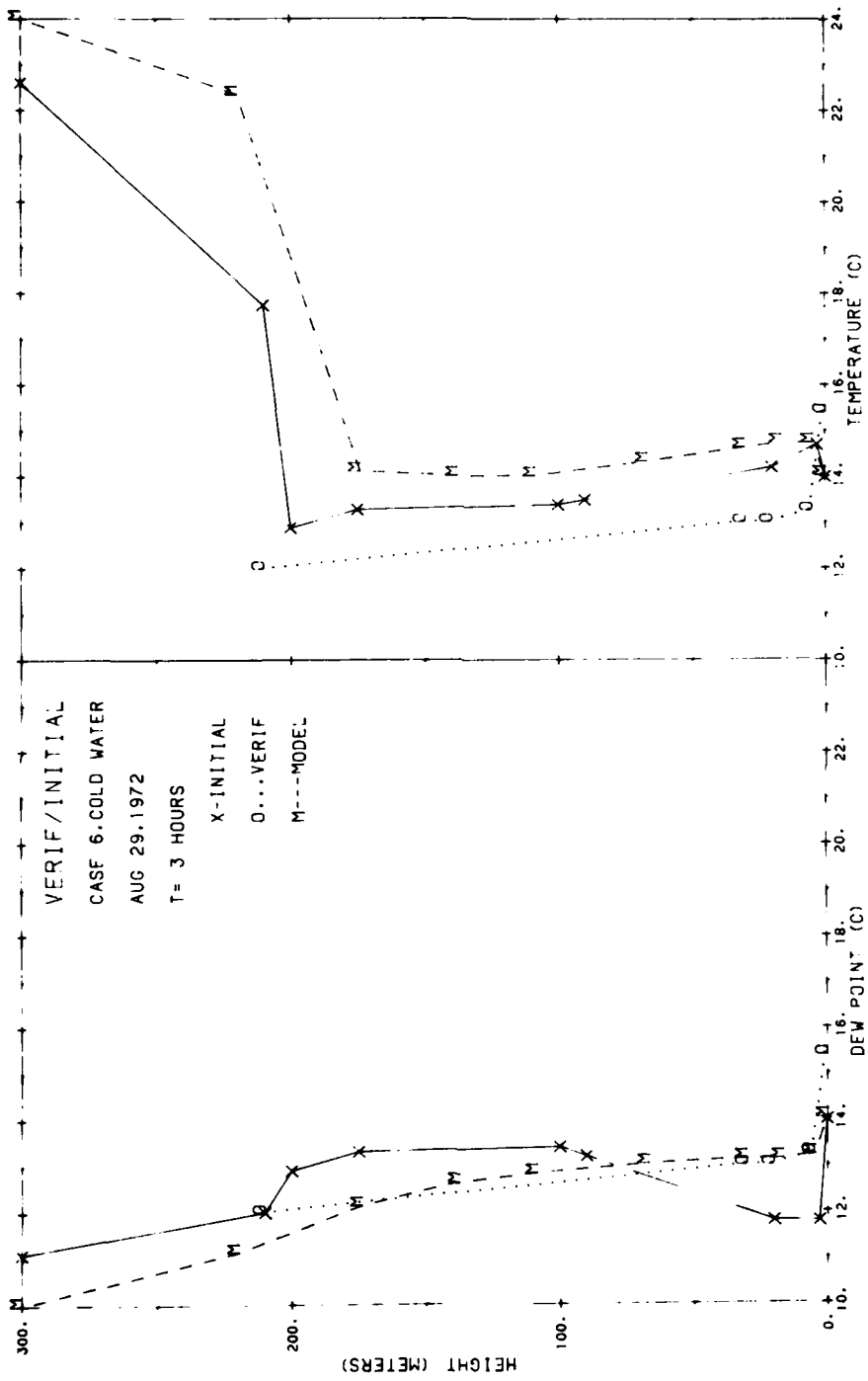

Figure A11. Initial, Verification, and Model Temperature and Dew Point Temperature Profiles for Calspan Case 6 at 3 Hours, Initial Cloud Layer. Sea surface temperature of 14.0°C

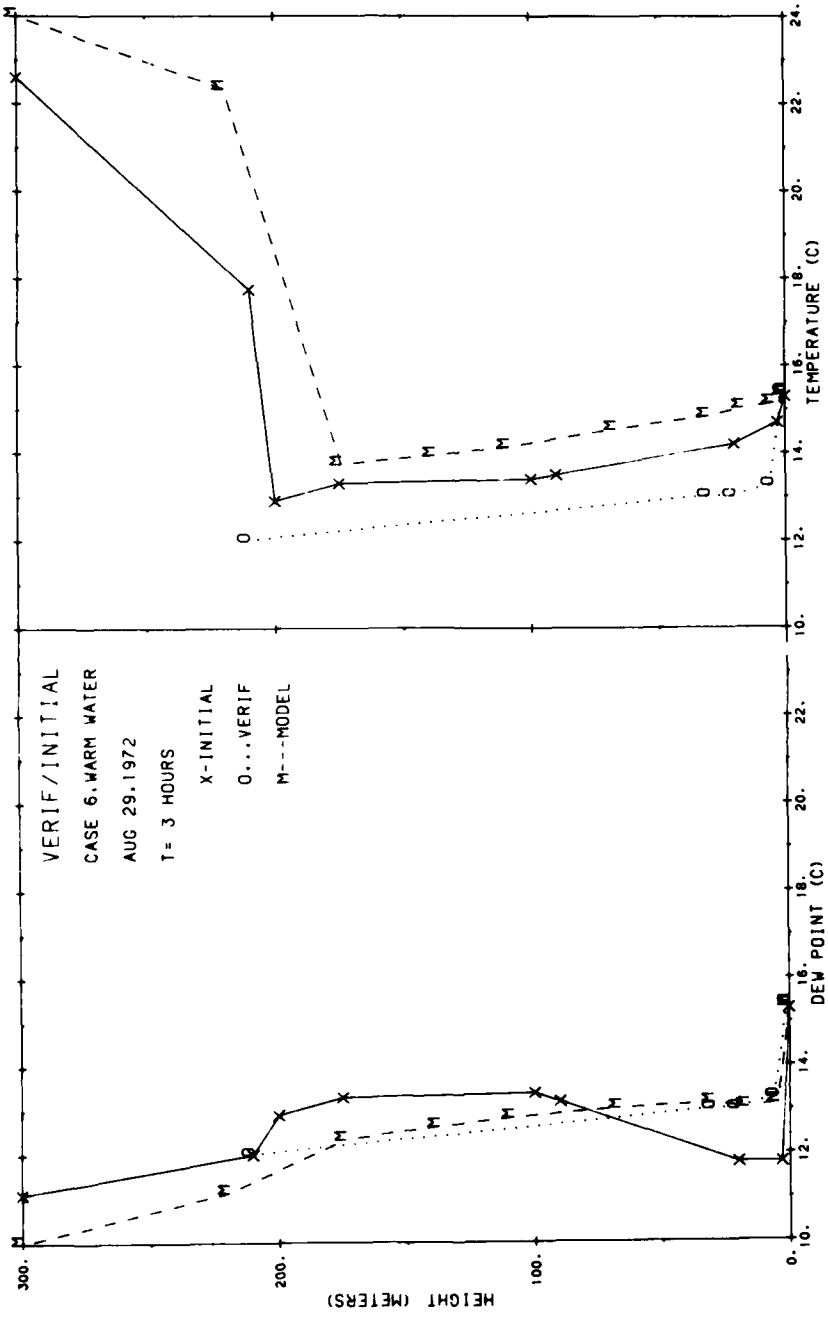

Figure A12. Initial, Verification, and Model Temperature and Dew Point Temperature Profiles for Calspan Case 6 at 3 Hours, Initial Cloud Layer Between 100 m and 200 m. Sea surface temperature of 15.3° C

END

FILMED

12-84

DTIC